(To be published in: The Physics of Highly and Multiply Charged Ions
Ed. F. J. Currell Kluwer Academic Publisher 2002)

Chapter 10

RADIOBIOLOGICAL EFFECTS OF HIGHLY CHARGED IONS

Their relevance for tumor therapy and radioprotection in space

Gerhard Kraft
Biophysik, Gesellschaft fur Schwerionenforschung,

Planckstr.1, 64291 Darmstadt, Germany

and

Technische Universitat Darmstadt

Key words: Linear Energy Transfer, ion beam therapy, relative biological efficiency, radioprotection in space, particle tracks, delta electron emission

Abstract: The radiobiological effects of highly-charged-ion beams are of interest for tumortherapy and for radioprotection in space. In tumor therapy, high-energy protons and carbon ions exhibit an inverse dose profile, i.e. an increase of energy deposition with penetration depth. This allows a greater tumor dose for protons and carbon ions than for photons. In addition, for the heavier carbon ions, this increase in dose is potentiated by a greater relative biological efficiency (RBE). On the other hand, the greater RBE of particles is the concern of space-radioprotection because the radiation burden of the cosmic galactic radiation consists of heavy charged particles from protons to iron ions. In this paper, the physical and biological basis of particle radiotherapy and its present status will be presented. For space radioprotection, the particle spectrum will be given and the risk of cancer induction and long-term genetic mutation will be discussed. In contrast to the cell inactivation problem for

tumor therapy, where physics-based models have been developed, the genetic changes are more complex in their mechanisms and only rough estimations can be given for the time being.

Table of Content

1. INTRODUCTION

Generally, radiobiology is mostly concerned with the influence of sparsely ionising radiation like x- or gamma-rays and electrons. In the last 50 years, however, the radiobiological action of heavy charged particles like protons or heavier ions has been studied with increasing intensity. This is for two reasons: first, heavy charged particles represent the best tool for an external radiotherapy of inoperable tumors. This is due to the favourable depth dose distribution where the dose increases with penetration depth and because of the small lateral and longitudinal scattering that allows irradiation of deep-seated target volumes with optimum precision. In addition, for particles heavier than protons, i.e. in the region of carbon, the biological efficiency increases at the end of the beam's range while it is low in the entrance channel, thus allowing a better inactivation of otherwise very radio-resistant cells of deep-seated tumors.

The second important field for particle radiobiology is the application in radiation protection in space research. In space outside the magnetic shielding of the earth, high-energy protons from the sun and heavier particles up to iron from interstellar sources pose a genetic and carcinogenic risk for man and can also influence and destroy semiconductor devices like computers. Because of the very high energies of these particles, shielding becomes difficult and extremely expensive. Therefore, the action of these particles should be known precisely in order to minimize the necessary shielding. In the following paragraphs, both problems will be dealt with in some detail but therapy will be paid more attention because of its greater relevance for our life.

2. PHYSICS RELEVANT FOR PARTICLE RADIOBIOLOGY

2.1 Microscopic Structure of an Ion Track

The knowledge of a particle beam's microscopic structure is essential for the understanding of the mechanism of cell inactivation and genetic effects [Kraft 1999]. The macroscopic dose of a particle beam, which is the main parameter in radiobiology, is given by the number of particles traversing the mass unit and the dose deposited by each particle, called linear energy transfer - LET. According to the Bethe-Bloch-formula the energy is

transferred to the target electrons that are emitted as delta electrons (High-energy delta electrons can form individual short tracks, called delta rays.) Measurements of delta-electron spectra revealed that more than three quarters of the dissipated energy is used for the ionisation process and only 10 to 20% are left for target atom excitation. Therefore, it is the action of the liberated electrons that - together with the primary ionisation – determines the biological action of the ions [Kraft 1993].

There are several processes that contribute to the features and the spectrum of the emitted electrons. For a high-energy transfer, the binding energy of the electrons can be neglected and electrons are treated as a free electron gas undergoing binary collisions. These electrons are emitted in radial symmetry around the centre of mass system that coincides with the projectile system because of the large mass excess of projectiles compared to electrons (figs. 2.1 and 2.2)

At lower energy transfers, the binding to the target atom becomes more relevant and the collision has to be calculated as a three–body interaction yielding a large number of electrons emitted with low velocity. At low particle energies, weakly bound electrons are exchanged with the target yielding a high–intensity peak at the velocity of the projectile. These are called Cusp-electrons because of the shape of the peak in the energy spectrum. At higher energies, this peak disappears because no electron can jump into bound states. Finally, Auger electrons from both, target and projectile atoms, can be emitted. The main characteristic of these emission processes is shown in a velocity plot in fig. 2.2 Most of the electrons are emitted in a forward direction.

For the calculation of the radial dose distribution around the particle track, the transport and energy deposition of these electrons has to be followed through the target material. The transport is characterized by elastic and inelastic scattering. While the elastic scattering changes only the direction, the inelastic processes i.e. ionisation and excitation can cause further biological damage.

The ionisation cross section has a maximum around 100 eV kinetic energy of the electrons. This maximum is almost independent from the composition of the stopping material as long as the material consists of organic compounds. There, the mean free path is in the range of 10 nm, which is about the dimension of DNA: high-energy electrons cause multiple ionisation events at the end of their range in a distance that corresponds to the cross section of a DNA molecule.

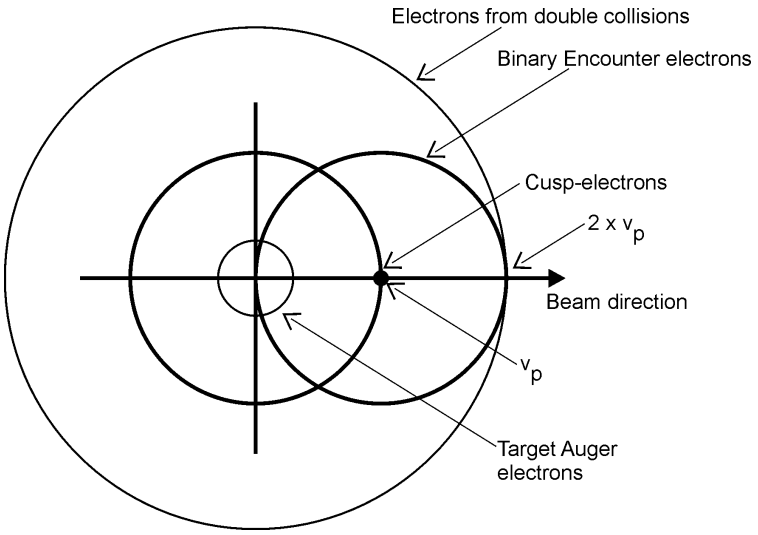

Figure 2.1. Velocity coordinates of the electron emission in ion-atom collisions.

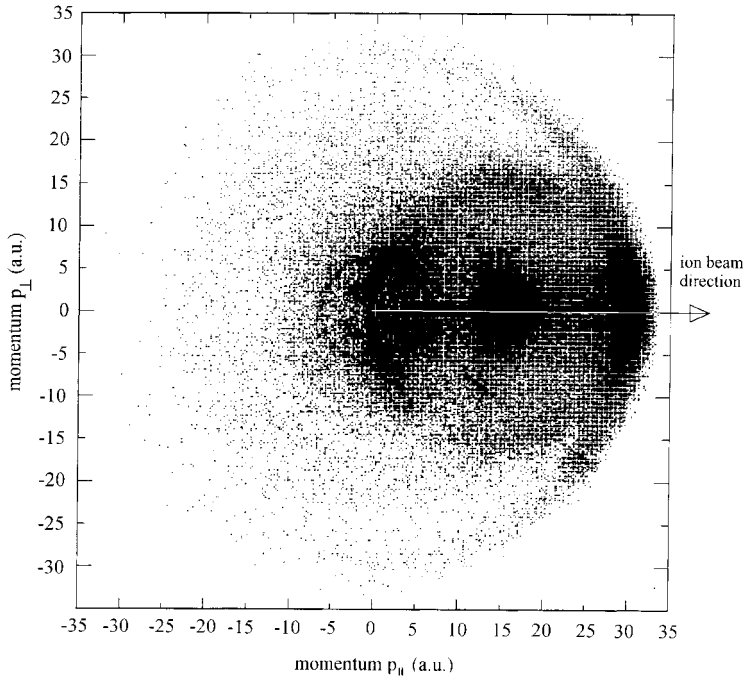

Figure 2.2:. Angular distribution of the measured electron emission [Reinold 1998]

As it makes no difference whether an electron is created by photon impact or by the impact of a heavy charged particle, there is no difference in the biological action of each individual electron either. There is, however, a big difference in the spatial distribution between electrons being created along a track of a heavy charged particle and the random distribution of electrons being created in photon beams and there is also a difference in ionisation density between particles of different energies and atomic numbers like protons and carbon ions.

For protons, mostly independent electron tracks are produced and the situation at the DNA level is similar to that of the photon-produced electrons: Locally correlated DNA damage can only be produced by increasing the total number of electrons i.e. by increasing the macroscopic dose. For the heavier carbon ions it is obvious that at low energies many electron tracks are produced that cause locally multiply damaged sites (LMDS) within the DNA. It is the reduced reparability of this clustered damage that causes the high relative biological efficiency (RBE) (see below).

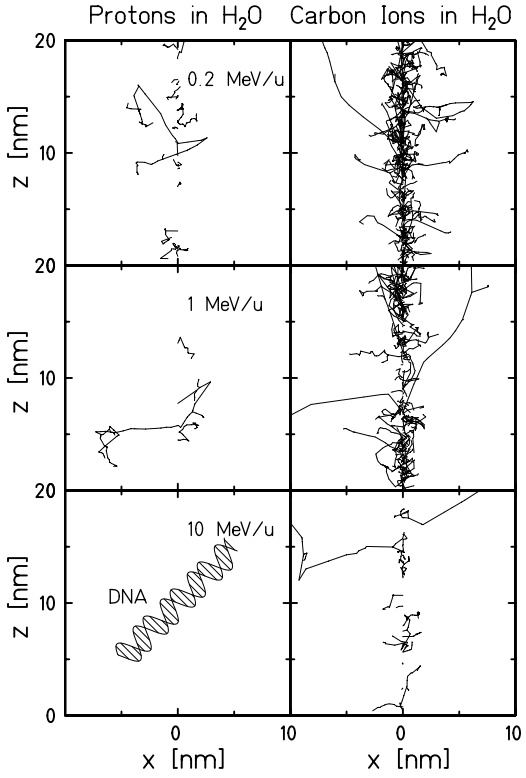

Figure 2.3. The microscopic structure of proton and carbon tracks in water is compared to a schematic representation of a DNA molecule. Protons and carbon ions are compared for the same specific energy before, in and behind the Bragg maximum [Krämer 1994]

2.2 Depth Dose Distribution (Bragg Curves)

The main reason to use heavy charged particles in therapy instead of photons is the inversed dose profile i.e. the increase of energy deposition with penetration depth up to a sharp maximum at the end of the particle

range, the Bragg peak, named after William Bragg, who measured an increase of ionisation at the end of the range of alpha particles in air [Bragg 1905].

This increase of dose with penetration depth for a particle beam produced by an accelerator was first reported by R. Wilson who recognized its potential for a medical application in tumor therapy [Wilson 1946].

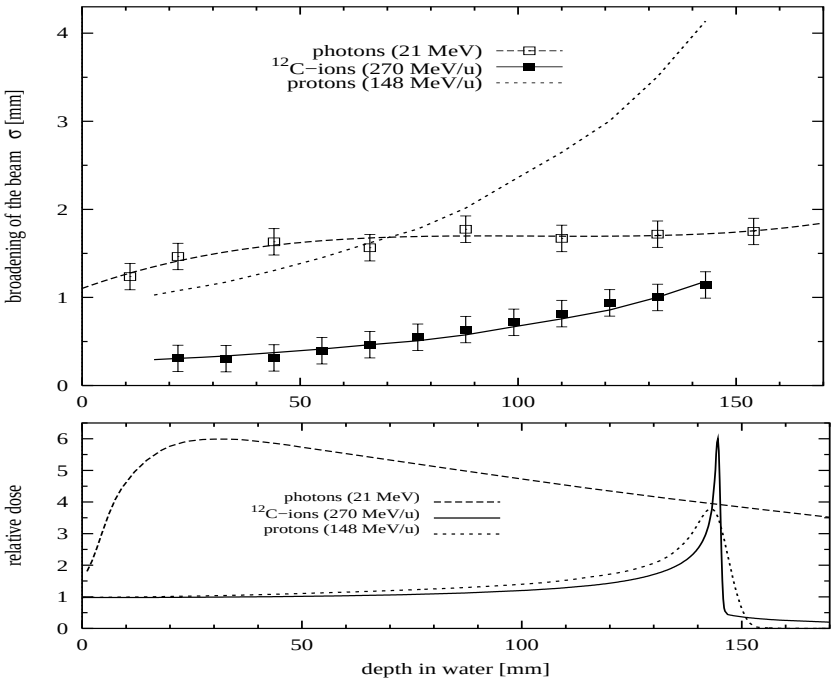

Figure 2.4. Comparison of the lateral scattering of photon, proton and carbon beams as function of the penetration depth (top) and the depth dose correlation (bottom) [Weber 1996]

The favourable depth dose distribution is a direct consequence of the interaction mechanism of heavy charged particles with the penetrated material and is different from that of electromagnetic radiation. Within the energy range used for therapy, heavy charged particles interact predominantly with the target electrons and the interaction strength is directly correlated with the interaction time. At high energies of the projectiles, the interaction time is short and the energy transfer to the target small. When the particles are slowed down and close to the end of their range the interaction time becomes larger and the value of the energy transfer is at its maximum.

The energy loss as function of particle energy and atomic number is given in the Bethe-Bloch-formula [Bethe 1930, Bloch 1933a, Bloch 1933b]:

$$\frac{dE}{dx} = \frac{4\pi e^4 Z_{eff}{}^2 N}{m_e \upsilon^2} \ln \frac{2m\upsilon^2}{I(1-ß^2)} + \text{relativistic} \qquad (1)$$

where m_e is the electron mass, υ the projectile velocity, N the density of the electrons of the target material, e the elementary charge and I the mean ionisation potential. Finally, Z_{eff} is the effective charge empirically approximated by Barkas [Barkas 1963]. For high energies, all electrons are stripped off the projectile and the effective charge equals the atomic number. At small energies, electrons are collected from the target and the effective charge decreases, yielding zero when the particles stop. The change of Z_{eff} is the main reason for the sharp decrease of the energy loss at lower energies, which is the essential criterion for the use of heavy particles in therapy.

2.3 Lateral and Longitudinal Scattering

When the energy loss is plotted over the penetration depth a Bragg curve for a single particle results in a dose ratio from plateau to peak of 1 to 2 orders of magnitude: Measured Bragg curves, however, have a much lower dose ratio because of the statistics of the energy loss process. The interaction of the projectile with the electrons is a process of very many collisions and most of the differences in the individual energy transfer are compensated but yield a small straggling of the particle range [Molière 1948, Gottschalk 1992].

Range-straggling broadens the individual Bragg curve and decreases the peak to plateau ratio. Because this process strongly depends on the atomic number of the projectiles, the Bragg peak is always broader for protons than for carbon ions. As a matter of fact, this is rather irrelevant for therapy because the tumors to be treated are larger than the natural width of the Bragg peak and various methods are now being used to extend the Bragg region over the size of the target volume. Only at the distal side of such extended or smeared-out Bragg peaks (SOBP) the natural decay is visible. Fig. 2.5 compares the extended Bragg peaks of protons and carbon ions at different penetration depths.

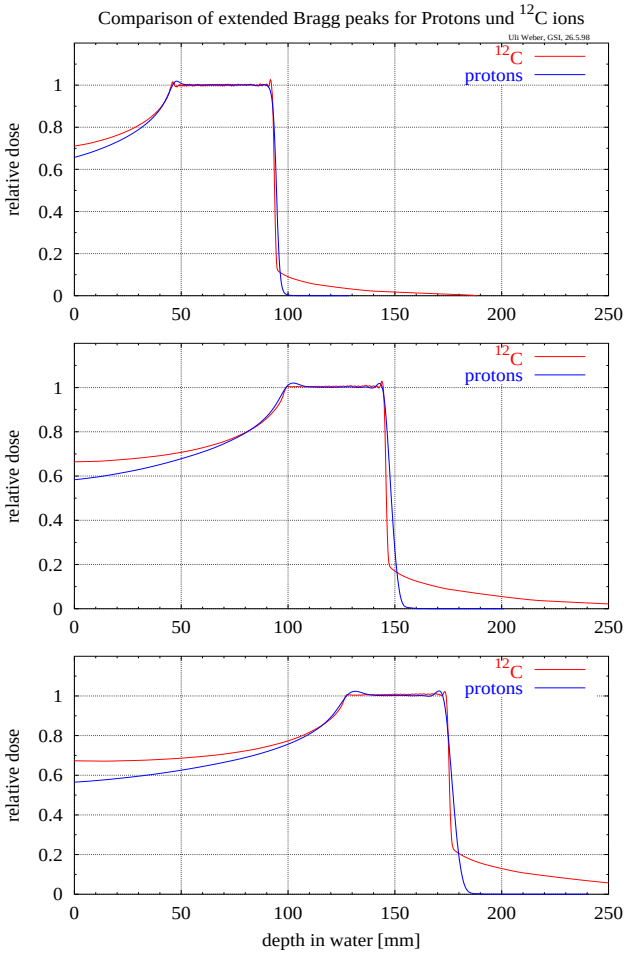

Figure 2.5. *Comparison of calculated extended Bragg peaks of protons and carbon ions at different penetration depths*

The differences between protons and carbon ions in the entrance channel as well as at the distal side are small. More important than the longitudinal straggling for therapy is the lateral scattering. In practical applications, a target in the proximity of a critical structure will not be treated in such a way that the beam stops in front of the critical site because of possible range uncertainties. These tumors are treated in a way that ensures that the beam passes the critical sites. Then, the lateral scattering determines the closest approach possible. Fig. 2.4 shows that for protons the beam broadening is less than the photon value of 2 mm for a penetration depth up to 10 cm in tissue. For carbon ions, the broadening is smaller than for photon beams up to a penetration depth of 20 cm. This is why extremely accurate fields can be produced with carbon beams also for deep-seated tumors while for more superficial tumors e.g. in the eye the accuracy of protons is sufficient.

2.4 Nuclear Fragmentation

A very important feature of particle beams is their nuclear fragmentation. When heavy ions pass through a thick absorber like the human body or a thick shielding of a space craft even small cross sections for nuclear reactions produce a significant amount of lighter reaction products. In radiotherapy the change in biological efficiency between the primary ions like carbon and the lighter secondaries has to be taken into account in treatment planning, as well as their longer range. However, radioactive positron-emitting isotopes are very useful to track the beam path inside the patient. For space research, fragmentation represents a major obstacle: In order to shield against the very numerous low-energy particles of a few hundred AMeV, very efficient energy absorbers are needed, in which the few high-energy particles produce showers of light low-energy particles. It has been calculated that an increase of shielding material does not necessarily mean a decrease in exposure. For high-energy heavy ion collisions, it is the pure geometry that mainly determines the reaction: For the more probable and therefore more frequent distant or glancing collisions, the majority of the projectile and target nuclei are not affected by the nuclear reaction. But in between, a zone of high "temperature" is created that can be deexcited by the evaporation of a few nucleons. Because of the reaction kinematics the lighter fragments have the same velocity as the primary ions at the collision [Hüfner 1985, Friedländer 1985]. The range of these fragments is given by the formula:

$$R_{fr} = R_{pr} \frac{Z_{pr}^2}{M_{pr}} \bullet \frac{M_{fr}}{Z_{fr}^2} \tag{2}$$

with R being the range, Z the atomic number and M the masses of fragments (subscript *fr)* and projectiles (subscript *pr)*, respectively. According to this formula, the fragments with a lower atomic number have a longer range. Because all lighter fragment nuclei may be produced - from the primary nucleus down to protons - these nuclei form a tail of dose beyond the Bragg maximum of the primary beam.

2.5 Positron Emission Tomography

When the carbon projectiles have lost one or two neutrons yielding ^{10}C or ^{11}C these carbon isotopes have a shorter range and stop before the stable ^{12}C-isotope. The neutron-deficient isotopes are of special interest for therapy because they are positron emitters and their stopping point can be monitored by measuring the coincident emission of the two annihilation quanta of the positron decay. Another positron emitter is ^{15}O, which again can be produced by nuclear reactions of carbon or protons inside the patient's body [Enghardt 1992]. To date, only positron emitting isotopes induced by carbon beams have been used for beam verification. Although the pattern obtained by positron-emitting isotopes is not identical with the dose distribution it is possible to monitor the range of the primary beam [Enghardt 1999]. This is very useful information because a critical point in any particle treatment is the proper calculation of the particle range. According to the Bethe-Bloch-formula the energy loss and consequently the particle range critically depend on the density of the material traversed. In the human body, there are density differences between fat, bone, and muscles of some thirty percent. A special problem for treatment planning are air-filled holes like those in ear and brain, that have a much lower density (fig. 2.6).

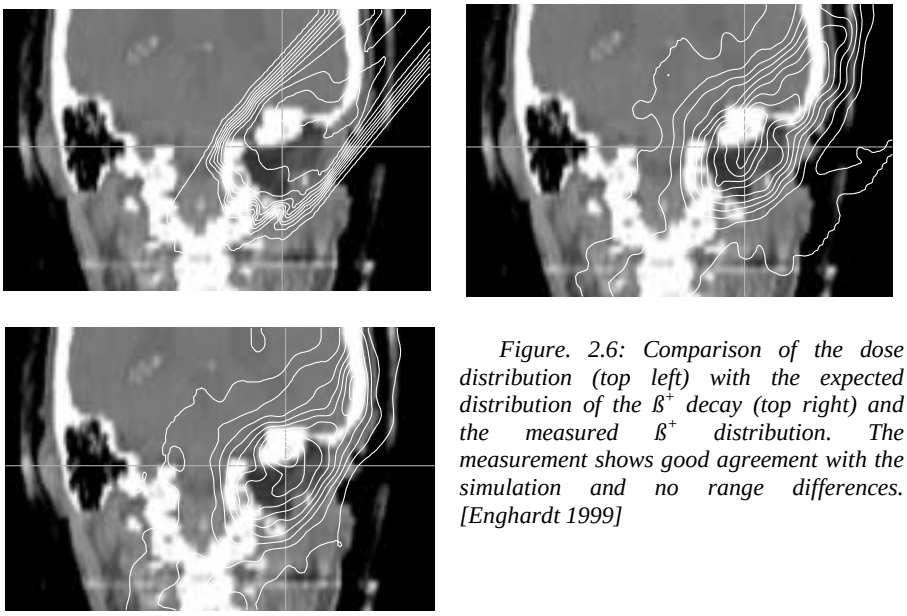

Figure. 2.6: Comparison of the dose distribution (top left) with the expected distribution of the ß$^+$ decay (top right) and the measured ß$^+$ distribution. The measurement shows good agreement with the simulation and no range differences. [Enghardt 1999]

3. THE RELATIVE BIOLOGICAL EFFECTIVENESS

3.1 Definition of RBE and its Dependence on Dose, Atomic Number and Repair

The problem of radiation therapy is to effectively kill tumor cells while protecting the normal tissue as far as possible. First, this is a problem of dose delivery precision and second, a biological problem to optimize the biological efficiency of the radiation to be used [Wambersie 1989].

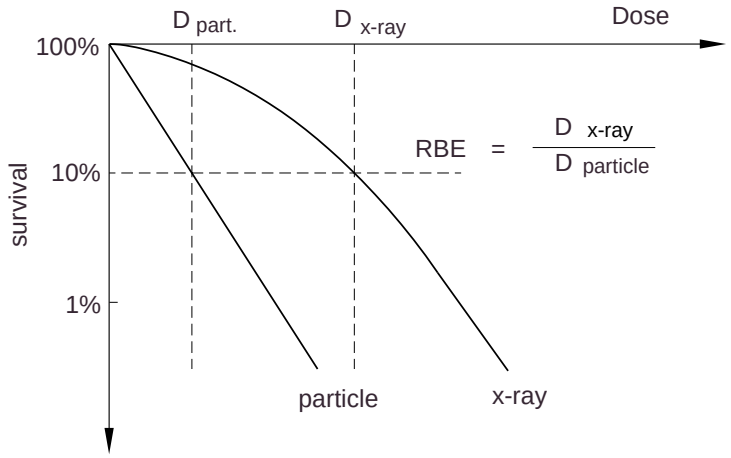

Figure 3.1. Definition of the relative biological effectiveness RBE, illustrated for cell survival curves

Experimentally it is found that densely ionising radiation like α-particles or heavier ions generate a greater biological effect than the same dose of X-rays [Kraft 1997]. In fig. 3.1 a schematic dose effect curve for cell inactivation for particles is compared to that of X-rays. The X-ray dose response is characterized by a biphasic behaviour: at low doses it has a large shoulder and at high doses a steep exponential tail. In practice, this graph can be approximated by a linear-quadratic response curve because of the limited - mostly low - dose range.

$$S = S_0 \exp - (\alpha D + ßD^2) \quad (3)$$

S/S_0 is the ratio of survival, α and ß are fit parameters that describe the response to the dose D. For particles, the quadratic compound decreases with increasing ionisation density and then the "survival curve" is characterized by a pure exponential decay with dose.

In order to compare the different radiation qualities the relative biological efficiency is defined as the ratio of X-ray dose to particle dose in order to achieve the same biological effect

$$\mathrm{RBE} = \frac{D_x}{D_{ion}} \quad (4)$$

with D_x and D_{ion} being the X-ray and ion doses, respectively. Because of the non-linearity of the X-ray curve, the RBE - according to this definition - is no invariable value, characterising the biological action of a particle beam in relation to photons. In fact, RBE strongly depends on the effect level and is greatest for lower doses and decreases with higher doses [Kraft 1996]. At very high doses, X-ray and particle response curves are usually parallel leading to a biologically optimized treatment plan that is only correct for one dose level. If the doses are changed in order to increase or decrease the effect, the biological optimisation has to be redone.

DNA is the main target for cell inactivation by ionising radiation. Therefore, all those dependencies of RBE on the various parameters become at least qualitatively evident from the mechanisms of DNA damage: at low X-ray doses, mainly isolated damage such as single strand breaks, etc. is produced. The cell has a very efficient repair system for this type of damage that occurs very frequently and is not only caused by ionising radiation. Even simultaneous damage at both DNA strands, i.e. double strand breaks, can be repaired by the cell rather quickly with a reduced but still high fidelity. But if the local damage is enhanced by higher local doses more complex DNA damage (clustered damage) is produced which is less reparable. This is visible in the steep decay in the X-ray survival rates at higher doses. There, the increment of biological damage is larger for the same dose than at low X-ray doses (fig 3.1).

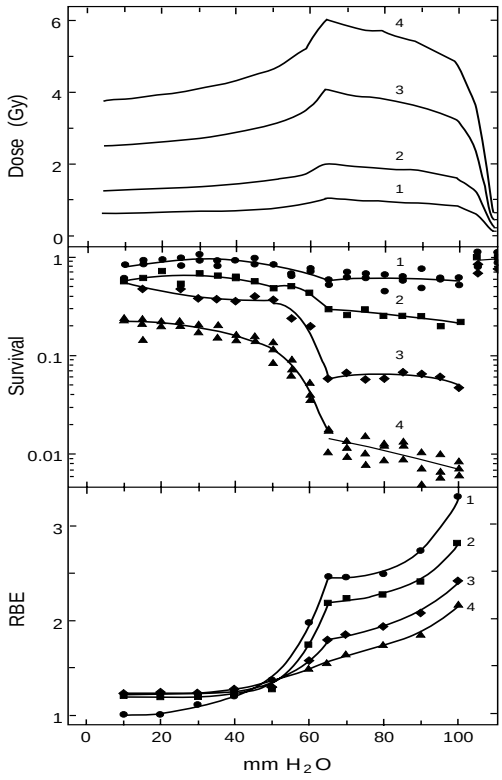

Figure 3.2 compares absorbed dose distribution (top), cell survival (middle) and extracted RBE values (bottom) for the carbon irradiation of a simulated 4 cm tumor 8 cm in depth. All dose values show an increase of RBE with penetration depth.

Another way to increase the local dose is the use of particles. For particles, high local doses are already produced in the centre of a single ion track (fig 2.5). For light ions like protons, only at the very end of the track i.e. at the last few micrometers, a clustering of DNA damage can be realized. This seems not to be of major importance for therapy. For protons, a small increase of RBE of 10 % is used throughout clinical therapy. Very heavy ions - argon or heavier - are extremely efficient in cell killing but unfortunately the efficient region also extends into the normal tissue in front of the tumor, causing heavy late damage. For ions between proton and argon, in the region of carbon, the RBE dependence is very favourable for therapy (fig. 3.2). At high energies, the local ionisation is low. Therefore, individual DNA lesions are produced with a large repair potential and the damage produced in the normal tissue in front of the target is as reparable as it is for X-rays. This yields an RBE of 1. At the end of the carbon ions' range, in the last centimetres, the local ionisation density reaches a level where a majority

of irreparable DNA damage is produced in a single particle track yielding high RBE values and efficient tumor inactivation.

There, RBE values up to three or four are found and the absorbed dose D as given in Gray has to be replaced by the effective dose (D_e) given in Gray-equivalent (Gye)

$$D_e\,[\text{Gye}] = D\,[\text{Gy}] \times \text{RBE} \tag{5}$$

The comparison of beams of different dose levels reveals the dose dependence of RBE. But for the practical application these data cannot be transferred directly to treatment planning. Provided RBE is mainly determined by DNA repair, the intrinsic repair capacity of the different cells plays an important role in the RBE effect. It has been shown experimentally that cells having little or no repair capacity exhibit little or no RBE increase when exposed to densely ionising radiation [Weyrather 1999]. On the other hand, tumors that are usually very radio-resistant because of their enhanced repair capacity become very sensitive to heavy ion exposure because of the larger RBE effect. It should be mentioned that the RBE dependence on atomic number has also to be taken into account with regard to the dose contributions of the lighter fragments produced by the carbon ions.

In summary, the increase in the relative biological efficiency, RBE, depends on the physical side of the track structure with high local ionisation densities causing clustered lesions. In addition, RBE depends on the intrinsic repair capacity of the tissue and shows the largest effect for conventionally radioresistant tumors.

3.2 Tailoring RBE for Therapy

The RBE determines the weighting factors for the superposition of the various Bragg curves in order to achieve a homogeneous killing effect over the complete target volume. The influence of RBE on the treatment plan very much depends on the method used for beam shaping. Using passive beam shaping systems the RBE dependence has to be in-built in the shape of the range modulators and is fixed [Chu 1993]. For active beam shaping systems the higher conformity with the target field has the consequence that RBE varies over the complete target volume in three dimensions [Jäkel 1998].

Due to a gain of knowledge in time, RBE has been determined in a different way at each of the three heavy ion centres: Berkeley, Chiba and Darmstadt. At Berkeley, *in vitro* data from cell cultures were used for RBE determination. In many experiments, cell survival was determined in pristine and also in smeared-out Bragg peaks of variable depth and width. These

measurements were used to design a set of ridge filters for the therapy of the tumor sites in the corresponding depth and extension. However, the implicit assumption is that these *in vitro* data of special human cell lines should be valid for all the human tissue affected by irradiation [Blakely 1980].

At the National Institute for Radiological Science (NIRS) in Chiba, a different strategy for the incorporation of RBE into the ridge filter design was used [Kanai et al.1997, 1999]. Again, the basis were cell experiments using human salivary gland HSG cells. Survival was measured for HSG-cells and fitted to a linear-quadratic dose dependence. For a mixed radiation field, the fit co-efficients were interpolated as function of LET. Thus, a nearly universal profile of the spread-out Bragg peak (SOBP) could be obtained for different carbon energies and different widths of the SOBP. With this universal ridge filter a flat survival response of HSG-cells could be produced independently from carbon energy but again, differences were found for other cell lines. Another important relationship was found in the experiments: RBE in the mid of the SOBP of carbon ions was close to that found in the experiment with neutron irradiation. Consequently, the dose prescription and fractionation at Chiba was adapted to the large clinical experience of neutron therapy [Tsujii 1996].

At GSI, the RBE is calculated separately for each voxel of the treatment volume. In contrast to the other facilities RBE is not deduced from in-vitro data. Instead, known X-ray sensitivities of the same tumor histology are the basis of the calculation. These data can be dose-effect curves for the specific tumor types or fractionation curves from which the X-ray sensitivity can be deduced. The basis for the calculation is the Local Effect Model (LEM) [Scholz 1997] where the RBE is calculated according to the size of the cell nucleus, the radial dose distribution and the X-ray sensitivity curve. In this model, the biological response to particle radiation is the convolution of the induction probability of lethal damage as measured with X-ray irradiation with the different values of the radial dose distribution integrated over the size of a cell nucleus [Scholz 1994].

$$S_{ion} = e^{-N_{lethal}} \tag{6}$$

with

$$N_{lethal} = \int_V \frac{\ln S_x(D)}{V} \bullet dV \tag{7}$$

being the number of lethal lesions, $S_x(D)$ the X-ray dose effect curve for cell killing, V the nuclear volume in the cell and S_{ion} the calculated survival after ion exposure. The surviving fraction for irradiation with a particular ion of various energies can be calculated if the X-ray effect is known. The RBE

is known for each volume element separately yielding a map of RBE values over the complete irradiation volume.

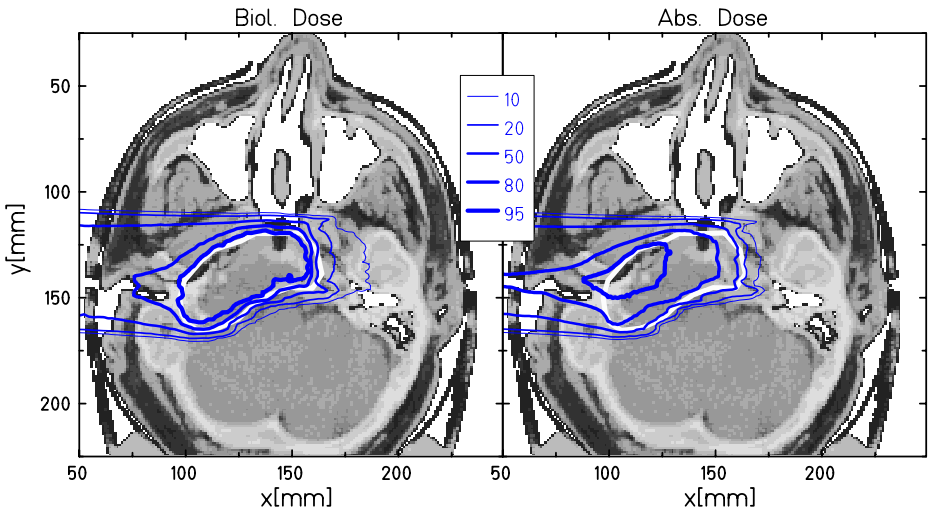

Figure 3.3: Comparison of the absorbed dose with the biologically effective dose for a tumor in the base of the skull. The biological effectiveness is increasing towards the distal end of the target volume. Therefore, a lower absorbed dose yield the same biological effect.

Figure 3.3. shows the biological and physical dose of a tumor in the base of skull. Beside the differences in the dose contours it is important that the physical dose is 0.5 Gy in its maximum while the biological dose is almost 2 Gye. Thus, RBE values up to 4 are applied to this slowly growing tumor.

The clinical experience with the patients treated at GSI with the biologically optimized dose profiles calculated according to LEM confirms the reliability of the calculations. Up to now, no recurrent tumors have been observed in the treatment field indicating the application of the correct RBE values [Debus 2000]. In summary, the RBE of the carbon beam is favourable compared to that of protons and represents an additional advantage in the improvement of the efficiency in tumor cell inactivation. This means at the same time that the very efficient carbon beams have to be applied with the utmost care in order to avoid any damage to the patient.

4. HEAVY PARTICLE THERAPY

4.1 Motivation for Particle Therapy

The term *cancer* stands for a large variety of diseases that have in common that cells of patient have lost their growth regulation and start to proliferate in an uncontrolled way, thereby producing a tumor. For benign tumors, this tumor growth stays local resulting in a single but ever enlarging tumor volume. In malign tumors, cells are spread throughout the body, seeding new tumor colonies everywhere, the so-called metastases.

The understanding of origin and mechanism of tumor diseases has made large progress with the discovery of the oncogenes and their behaviour on the microscopic level. But up to now, this knowledge is not sufficient to cure tumors. In contrast to a bacterial infection, where foreign cells invade the body from the outside and can be destroyed because they are different from the host's body cells. The growth of a tumor is the growth of oncogenetically deregulated but otherwise normal cells of the respective patient. In addition, oncogenes are also present in the non-tumor cell, i.e. in all normal cells controlling cell growth. But their influence on cell growth normally comes to a halt when the organ has reached its genetically determined volume. Not so tumor cells.

Up to now, it has been impossible to destroy a macroscopic tumor with molecular methods although large effort is being made in this direction and great hope is put on this field. At present, the most efficient way to kill a tumor is to remove it by surgery as long as the tumor is small and solid i.e. not metastatic (fig. 4.1). Chemotherapy uses drugs to stop proliferating cells i.e. tumor growth in order to extend the patient's life. Finally, a large fraction of tumors can be eliminated by radiotherapy with ionising radiation. In principle, any tissue can be destroyed by radiation if only the dose is high enough. In practice, the dose that can be given to a tumor is limited by the tolerance of the normal tissue surrounding the tumor and the normal tissue dose is determined by physical parameters, e.g. the depth dose dependence and the lateral scattering of the radiation.

Conventional therapy started with low-energy X-rays. In order to increase the precision of the delivered dose electromagnetic radiation such as ^{60}Co-gamma rays and finally bremsstrahlung photons from linacs were used because of the smaller scattering and the increase of dose for the first three centimetres followed by an exponential decay with depth. An entirely different behaviour can be expected from heavy particles. For heavy ions the dose even increases with depth and lateral scattering can be minimized.

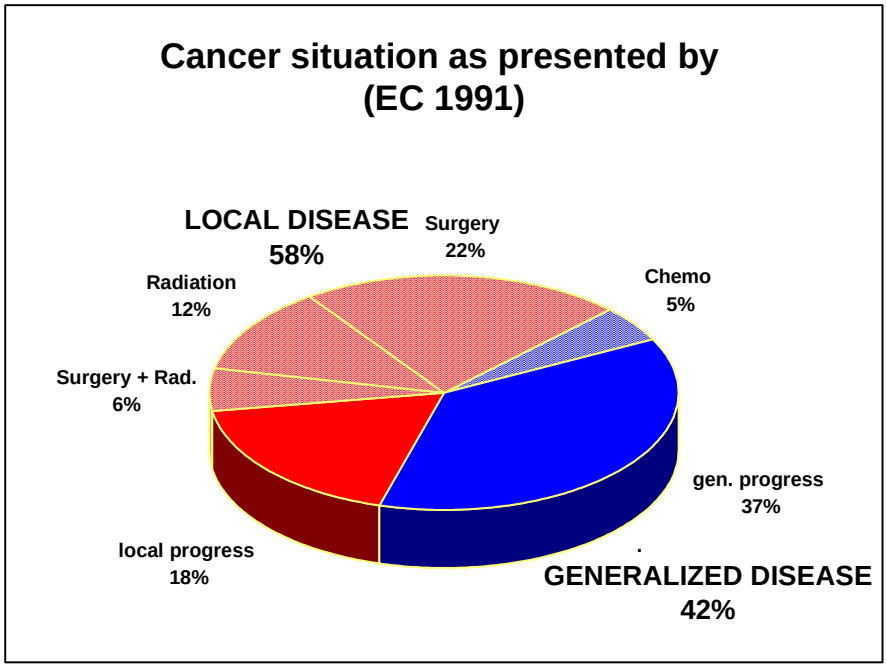

Figure 4.1. Distribution of the approximately 1 million new cancer patients of the European Union per year. Patient diagnosis with local diseases i.e. one single primary tumor has a greater chance for a long-term cure by the various treatments.

A second strategy for a higher irradiation efficiency in the tumor was to use radiation of different "biological quality". This was attempted in a neutron therapy where an almost threefold biological effect can be found for the same absorbed dose. Neutron therapy produced an excellent tumor control because of the elevated relative biological efficiency (RBE). However, these positive results were correlated with severe side effects due to the very poor depth dose profile of neutrons. Thus, the high efficiency for tumors also affects the normal tissue surrounding the tumor.

In contrast, heavy charged particles in the region of carbon produce a high RBE which is comparable to that of neutrons but which is restricted to the end of the particle range. Therefore, tumor cells can be killed with greater efficiency but the normal tissue in front of the tumor is not exposed to high RBE radiation. For these reasons – a very high precision in dose delivery and a greater biological effect which can be restricted to the tumor – heavy ions promise a much better cure rate.

Heavy particle therapy is predominantly applied to deep-seated tumors where the advantage of the inverse dose profile is most significant. In

general, the size of the target volume is much larger than the spot of an unmodified beam as produced by the accelerator. Therefore, the beam has to be enlarged laterally and longitudinally. In the beginning of particle therapy in the sixties and seventies, passive beam shaping devices were developed in which the beam is distributed at each instant over the complete target volume. These mechanical devices had the great advantage of simplicity and of not being sensitive to intensity fluctuations from the accelerator. But passive systems had to be tailored individually for each patient and even then the congruence between the optimum target volume and the actually irradiated volume was not satisfying.

Active systems make use of the possibility to deflect a beam of charged particles by magnets and to change its range by energy variation of the accelerator. With active systems, a most conform beam delivery can be achieved without patient-specific hardware. But active systems require a more sophisticated control system, which only became possible after more powerful computers had become available. Active systems are more sensitive to accelerator fluctuations but offer great flexibility and do not need patient-specific hardware.

4.2 Passive Beam Spreading Systems and Intensity-Modulated Particle Therapy

For a passive shaping of the ion beam, many hardware variations exist that cannot all be described here but are reported in great detail in [W. Chu, 1993]. For the lateral enlargement, scatter systems as given in fig 4.2 have been used. In order to avoid beam fragmentation in passive devices, magnetic deflection systems like wobblers or scanners have been introduced but these magnetic deflection systems had no feedback to the beam delivery from the accelerator. Homogeneity over the target area was achieved by repeating the deflection pattern so many times in a random way that all fluctuations in the beam intensity were averaged.

In order to shape the beam in longitudinal direction absorbers of variable thickness were introduced. These absorbers consist of regions of different thickness. A part of the beam penetrates a thicker absorber having then a short range in the patient while another part penetrates a thin absorber having a longer range in the patient. This principle has been realized in many ways as for instance in linear or spiral ridge filters or in propellers of different thickness.

Finally, the distal part of the target field can be shaped by compensators or boli in front of the patient in order to spare critical structures behind the target volume. This shaping, however, is done at the expense of an extended high-dose field in front of the target volume (fig. 4.2).

In summary, passive systems allow only a limited adaptation of the irradiated field to the target field and in order to exploit the advantages of heavy charged particles to a full extent active systems are indispensable.

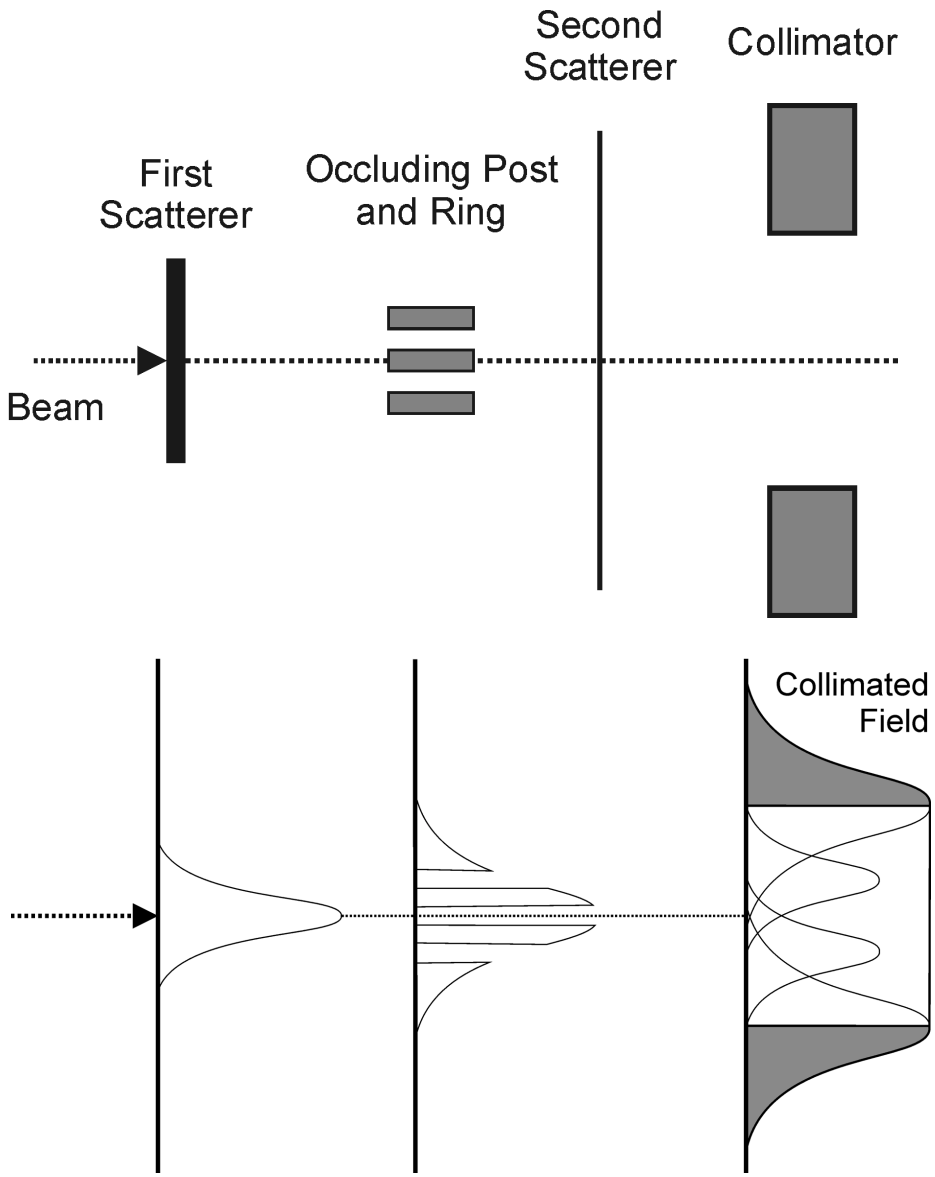

Figure 4.2: Passive beam shaping system to produce a flat dose distribution over a large field. Uniform fields are produced by a first scatterer and an annular ring plus a second scatterer. [redrawn according to Chu 1993]

In order to reduce the unavoidable waste of the primary beam when using passive systems and to reduce the fragmentation of heavy-ion beams active lateral scattering systems have been developed mostly at Berkeley [Chu et al 1993]. In these systems, magnets that are perpendicular to each other and to the beam axis deflect the ion beam. Two types of beam pattern have been realized - linear and zigzag - raster scanners and circular patterns (wobbler). In the linear system, two fixed triangle frequencies are used, for instance a slow one to move the beam up and down and a fast one to write horizontal lines similar to those in the TV-system. In the circular wobbler system, sinusoidal frequencies of the same amplitude are applied to the magnetic deflection system having a phase shift of 90° between horizontal and vertical deflection magnets. By selection of 3 different amplitudes, 3 different circular distributions that are stacked with the correct intensity are used to achieve a flat field larger than the treatment area. However, there is no feedback between the fluctuation beam intensity and the speed of the deflection. In order to achieve a homogeneous dose distribution the target field has to be covered many times with the hope to average out the inhomogeneities of the accelerator fluctuations.

Intensity-controlled scanning systems for 3 dimensions have been developed by PSI in Villigen for protons [Blattmann 1995] and by GSI in Darmstadt for carbon ions in order to achieve the best target-conform irradiation fields possible [Kraft 1991, Haberer 1993].

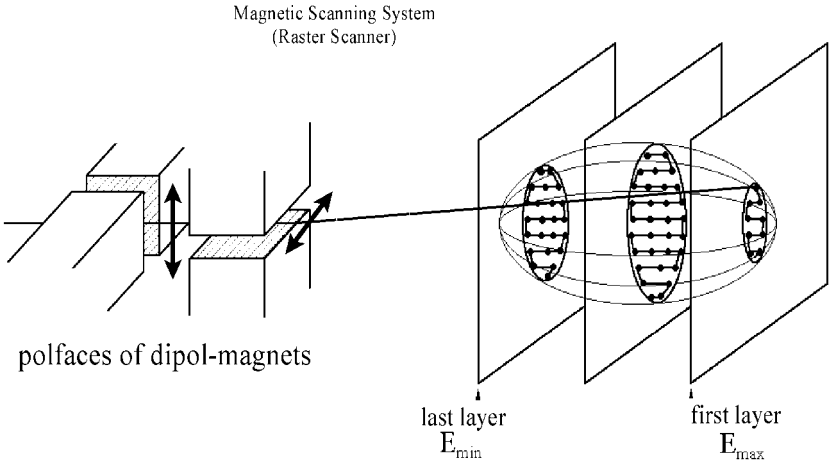

Figure 4.3*: Schematic drawing of the intensity-controlled rasterscan. The target volume is dissected into layers of equal particle range that are covered by a net of picture points. The beam is guided along the imaginary line of picture points by two fast magnets.*

The target volume is dissected into layers of equal particle range. Using two deflecting magnets driven by fast power supplies, a “pencil beam” is scanned in a raster-like pattern over the layers, starting with the most distal one. After this layer has been painted the energy of the beam and consequently the range is reduced and the next layer is treated (fig 4.3).

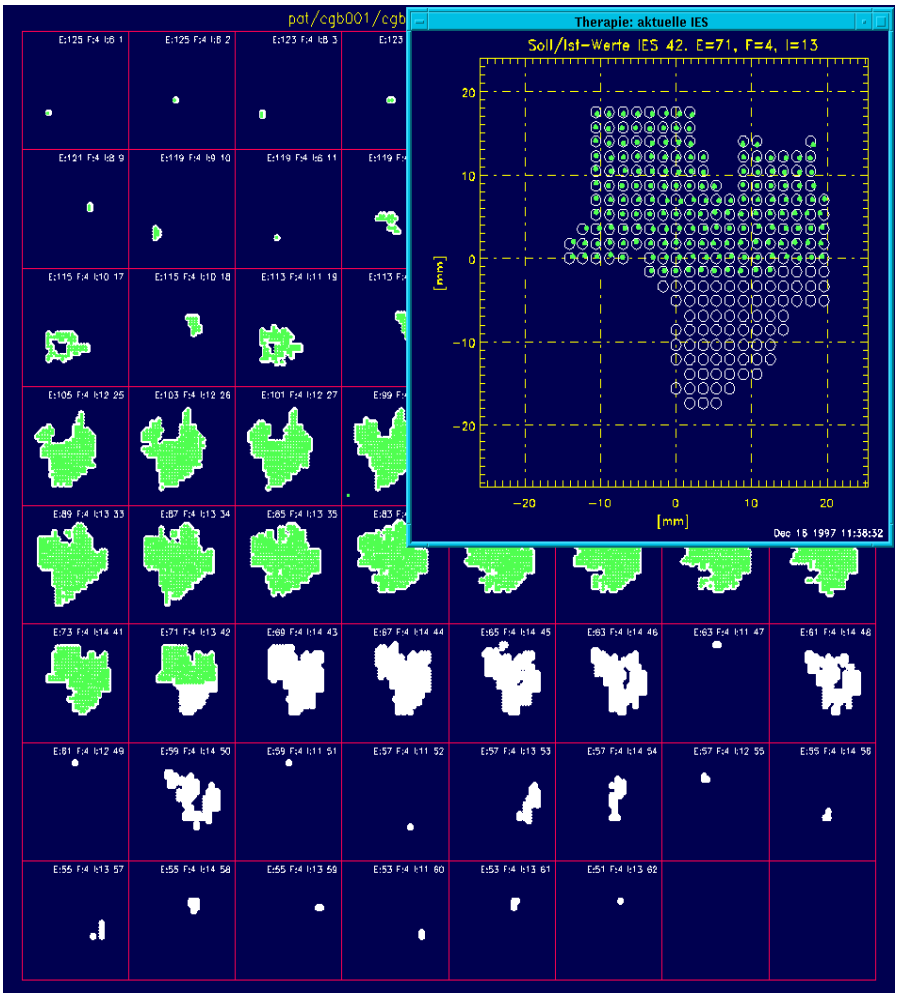

Figure 4.4 Compilation of the different range slices of a treatment volume. In each panel one slice is shown, in the magnified panel the circles represent the calculated centre positions of the beam that are filled with the measured centre of the beam. The beam diameter is larger than the circles and overlaps many positions yielding a homogeneous distribution [Brand 1998].

The difficulty arising from this method is obvious: the more proximal layers are already partly covered with dose when the distal layers are being

treated. Consequently, these layers have to be covered during the continued irradiation with an inhomogeneous particle distribution in order to reach a homogeneous dose distribution or a homogeneous distribution of the biological effect over the total target volume in the end. In order to achieve the desired inhomogeneity the beam path is divided into single picture points (pixels or voxels) over the individual areas for which the individual particle covering has been calculated before [Haberer 1993]. In this intensity-modulated particle therapy (IMPT), up to 30,000 pixels per treatment volume are filled with an individually calculated number of particles. Because of the finite range of particle beams the IMPT has an additional free parameter compared to similar X-ray techniques, called IMRT.

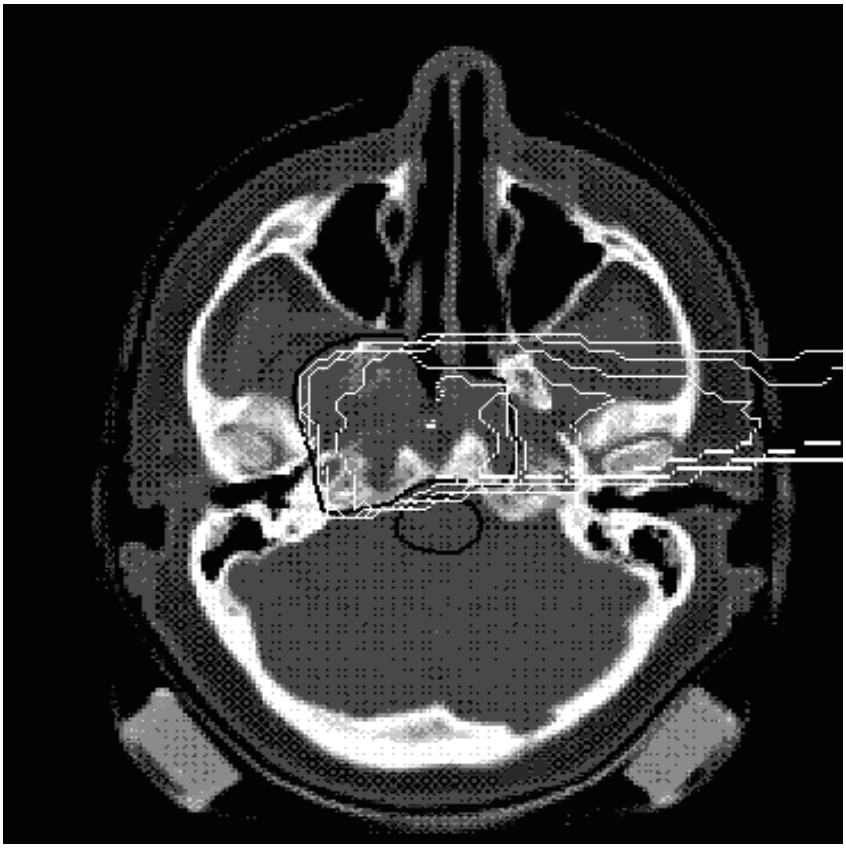

Figure.4.5: Computer tomography section through the head of a patient. The treatment plan is superimposed, showing isodose contours [Jäkel 1998]

Although each layer may differ in contour, the shape of a target volume can be "filled" with high precision. The different layers are of great

complexity as is shown in fig. 4.4 that depicts the energy slices of a plan of a patient treated at GSI with carbon ions.

The small spots of high or low energy ions in the beginning and at the end of scanning are due to the density inhomogeneities of the tissue. Small areas of high density like bones have to be treated with higher energies. This accounts for the small spots of higher energy irradiation. Vice versa, areas of low density have to be filled with low energy particles [Jäkel 1998].

In fig. 4.5, a final treatment plan is projected on a CT scan of a patient. The good conformity of target volume and treatment area as well as the steep gradients of the dose in areas adjacent to critical sites are visible.

4.3 Comparison of Beam Spreading Systems

Ion beam therapy with protons and heavier ions started in the late sixties when the stability of accelerators was rather poor and no sophisticated control system was available due to the lack of fast computers. In addition, in conventional therapy, during the transition from X-rays to Co-gamma rays at best tolerable dose distributions were achieved. Frequently, the tumor dose was not high enough to reach a permanent cure.

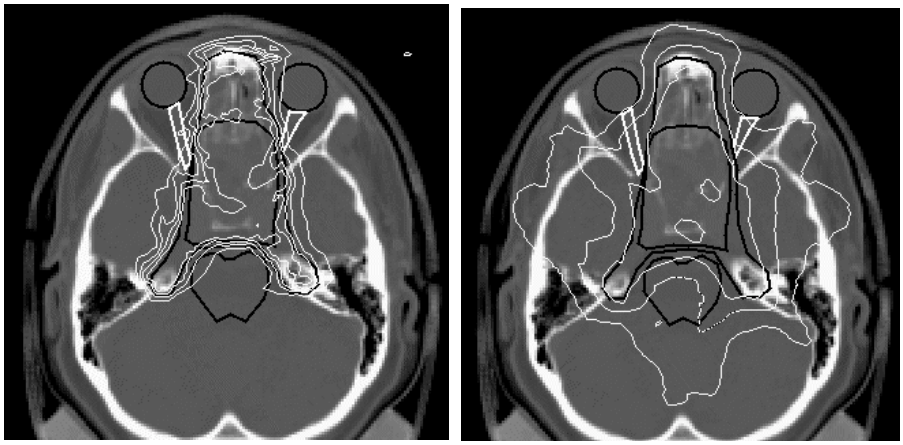

Figure 4.6. Comparison of Treatment Plans. Heavy Ions (left) 2 fields. IMRT (right) (With the courtesy of O.Jäkel, DKFZ Heidelberg)

Back then, the transition to the very advantageous inversed dose profiles of particles represented major progress. When using passive beam delivery systems the quality of the beam distribution is widely independent from the accelerator performance of the accelerator and from intensity fluctuations.

For small proton fields, like those for the treatment of eye tumors, the passive beam application still offers the best and cheapest solution.

For larger and deep-seated tumors the comparison becomes more difficult. Conventional therapy, however, has made large progress over the last years. Co-gamma units are widely replaced by electron linacs and sophisticated methods for treatment planning and beam delivery keep up with the meanwhile improved accuracy of diagnostic methods like CT, NMR and PET. Using intensity-modulated radiation therapy (IMRT) dose distributions very close to the target volume can be achieved that are comparable and sometimes even better than the ion beam application using passive absorbers [Verhey 1997]. Nevertheless, active particle beam application is always better in its conformity than any passive beam shaping method and also better than X-ray-IMRT. The scanning methods developed at PSI and GSI represent an optimum 3-dimensional type of "particle IMRT" since the beam intensity can be controlled not only for each direction but also for each depth position separately.

4.4 Treatment Planning

4.4.1 Static Fields

Prior to the development of tomographic methods the available information on the location and the size of a tumor was rather poor and based on a few X-ray images that gave the projection of the tumor volume only but not an exact 3-dimensional image. This poor visual information corresponded in some way to the limited possibilities to deliver the dose using X- or gamma-rays. In tomographic imaging, computer-assisted X-ray tomography (CT) came first, followed by positron emission tomography (PET) and magnetic resonance imaging (MRI), now allowing delineation of the contour of the tumor with millimetre resolution and in three dimensions.

In particle therapy, these images are used to deliver the beam in a most conformal way to the tumor volume. Thus, the first task of treatment planning is to identify the target contours that are usually larger than the tumor volume. It is the task of the physicians to graph the border lines in each slice of the tomogramme and to select the best possible entrance channels as well as to mark the organs of risk such as brain stem, optical nerves, eyeball, etc.. This procedure is independent from the type of radiation to be used. The next step of particle treatment planning very much depends on the system to be used for beam delivery.

For passive systems, the contour of the largest projection in beam's eye view is translated into a collimator to be mounted in front of the patient. A limited depth modulation is obtained by the deployment of ridge filters and

compensators or boli that will also be installed in front of the patient. For the design of these compensators, the density inhomogeneities in the penetrated tissue have to be known. In tissue, there are density differences between fat, bone and soft tissue up to 30% or 40%. In addition, “vacuoles” i.e. air-filled gaps or metal implants (as bone substitutes) exhibit even larger density variations. In general, the density can be obtained from the CT image: after calibration, the gray values of the CT can directly be translated into water-equivalent density values. Higher densities are then translated into a longer path in a water-equivalent target and correspondingly, lower densities are translated into shorter water-equivalent ranges. This translation is possible because the dose is defined as energy deposition per mass unit and the compression or the dilatation of the absorber material changes the energy loss proportionally to the density while keeping the dose constant. The translation into water-equivalent densities is the basis for the calculation of compensators for passive delivery systems and for the treatment planning in active beam delivery systems.

4.4.2 Inverse Treatment Planning

In active beam delivery systems, the target volume is dissected into layers of equal particle range and the beam is moved over these layers from pixel to pixel. Treatment planning for heavy ions is just “inverse” to this procedure. It starts from a pixel in the most distal layer and - in a first approximation - calculates the number of stopping particles necessary to produce the required dose. This is done for all pixels of this distal layer. Then, the next and more proximal layer is treated in the same way. In order to determine the correct dose, the fraction of the dose deposited during the irradiation of the deeper layer has to be subtracted. Thus, layer after layer is treated for the planning of the entire volume. Due to the fact that heavy ions have a dose tail beyond the Bragg maximum a few more steps are required before the absorbed (i.e. the physical dose) fits perfectly to the target volume.

If two or more entrance channels are used the planning can be carried out independently, generating a homogeneous field for each entrance channel. However, with regard to the geometry of the tumor, it is frequently more appropriate to plan inhomogeneous fields that will result in a homogeneous field if all entrance channels are used.

For heavy ions like carbon, further complexity arises from the variation of the RBE over the treatment field. In each volume element, the dose originates from a mixture of primary and secondary ions of different energies. Because the RBE depends on atomic number and energy, this mixture has to be known in order to calculate the local RBE values correctly.

After the optimisation of the physical dose local RBE values have to be calculated as weighting factors of the dose. Then, the irradiation field has to be re-optimized. As RBE also depends on the dose level, local RBE values have to be calculated iteratively in this second step and in all further steps of optimisation. In one treatment field, 10,000 up to 50,000 individual pixel points are irradiated and have to be optimized beforehand. Consequently, the final biological optimisation is far more time-consuming than the optimisation of the absorbed dose alone.

Because this planning starts from the dose to be delivered in different pixels to the target and calculates the number of particles and their energy to be delivered, this type of planning is called inverse planning or intensity-modulated particle treatment (IMPT). A similar method has recently been developed and is now being used in patient treatment with high-energy photons from electron linac bremsstrahlung. Here, the photon field from the accelerator is first restricted in its contours and the intensity in each point of the field is modulated with a variable collimator (multi-leaf collimator). Using photons with an inverse planning and delivery scheme, the so-called Intensity-Modulated Radiation Therapy (IMRT) a dose distribution can be produced that is very often comparable to that of a proton beam but requires less investment. However, the precision of a carbon beam cannot be reached with IMRT.

4.5 Patient Positioning

The fundamental advantage of particle therapy is the high precision of beam application. Up to now, the beam has been delivered in the frame of a coordinate system fixed with respect to the treatment room. Therefore, the patient has to be immobilized and adjusted within the same coordinate system. For this purpose, a large variety of techniques have been adapted from high-precision photon therapy like stereotactic treatment or IMRT [Schlegel 1993]. For the immobilisation of head and neck, thermoplastic masks and bite blocks are used. These devices are manufactured for each patient individually. Bite blocks allow a precision and reproducibility of 1-2 mm. Thermoplastic masks cover the head completely and allow a positioning accuracy better than 1 mm. For a total immobilisation of the body foam moulds and thermoplastic total body masks have been developed that guarantee accuracy almost to the millimetre. In any case, the position of the patient is checked prior to the treatment to an extent that correlates with the precision of the treatment. For passive beam shaping using proton beams this precision may be less than for active beam scanning with carbon ions where a precision better than 1 mm must be guaranteed throughout the entire treatment.

In the thorax, the external immobilisation is counteracted by the internal motions due to heartbeat and breathing. These motions are more or less cyclic and of regular amplitude. Up to now, the treatment of tumors in the lung has been "gated" with the breathing for passive beam shaping and the beam is applied only during a short period of time of relative stability. This procedure is not applicable for active beam scanning because of a drastic elongation of the exposure time as well as the possibility of residual interference patterns caused by small motions producing hot and cold spots. However, the active beam scanning is - in principal - able to follow patient motion if the scanning is significantly faster than the internal motion but it has not been realized to date.

First attempts to adjust the position of the patient's body directly to the irradiation have been made in NAC South Africa, mainly with the intention to correlate the initial position of the patient with the coordinate system of the beam delivery. For this purpose, light marks are fixed on the patient and monitored via a TV system. Because patient positioning is a very time-consuming and expensive part of any precision treatment major efforts for the improvement are being made in this field [Langen 2001].

4.6 Safety and Control System

It is the purpose of the safety and control system to ensure a safe and precise delivery of the prescribed dose to the target volume. In practice, very different systems for beam delivery are being used. Therefore, it is impossible to describe a general safety and control system for all therapy units [Alonso 1994, Renner 1995, Brand 1998, Wiezczycka 1999]. It is, however, common to all systems that they can be divided into an accelerator section and an application section.

Regarding passive beam shaping, these two sections are separated because the quality of the beam as extracted from the accelerator does not influence the quality of the application. As long as energy and atomic numbers are correct, the right beam shape is produced by the absorbers, range shifters, compensators, etc. The safety of the treatment only requires that the exact number of particles as measured in an ionisation chamber enters the system and that all necessary components are in the right place. Of course, the patient has to be positioned correctly, too [Chu 1993].

For an active beam delivery system, the interplay of scanning system and accelerator is more complex [Brand 1998, Kraft 2000]. First, the energy has to be changed stepwise without a change of the zero position of the beam and its diameter. Second, the beam extraction has to be smooth in time. Although intensity fluctuations can be rectified by the feedback of the scanning system, a "grass"-like structure with large intensity spikes makes

scanning difficult. In addition to the beam energy, the diameter of the beam in the target has to be changed on request from the scanner in a controlled way. For safety reasons, a monitor system has to be installed in front of the patient that controls these parameters independently. At the GSI scanner unit, the heart of the monitor system consists of two ionisation chambers and two multiwire chambers. The combination of a wirechamber and an ionisation chamber measures the position of the beam and its current intensity. This combination is read out 6,000 times per second and at least four times for each voxel. If more than one measurement per voxel disagrees with the requested number the beam is aborted in the accelerator within less than half a millisecond. In addition to this fast interruption cycle, slow monitor systems control other important parameters such as the vacuum in the beam pipes, gas flow in the monitors or access control and so on. Similar control and safety systems adapted to the respective needs of the beam application system are installed in all therapy units. It is, however, also common to all therapy projects that the required manpower for the system software is usually completely underestimated.

4.7 Gantry

The term “gantry” stands for a beam delivery system that allows one to administer the beam from all directions to the patient in a supine position. For conventional therapy using photon beams with the exponential depth dose distribution, the use of a gantry is mandatory for any treatment of a deep-seated tumor in order to distribute the large integral dose outside the tumor over a large volume.

In photon therapy, the radiation source or the electron linac is moved around the patient. In particle therapy, it is impossible to move the accelerator around the patient. Instead, deflection magnets are mounted on a turnable system. The most frequently discussed systems are given in fig. 4.7.

At Loma Linda, three corkscrew gantries are in operation for therapy. But at present the systems are not equipped with scanning. An excentric gantry including a voxel scan system has been built at PSI, Villigen, and three gantry systems are installed at the NPTC, Boston.

For carbon ions, no gantry system has been realized yet. Because of the greater ion energies necessary to obtain the same penetration depth and because of the higher magnetic rigidity the design of a carbon gantry cannot be a straightforward blow-up of a proton design. Recent proposals for carbon gantries at GSI use upstream scanning to reduce the gantry radius. But even

with this design the weight of the carbon gantry would be about 600 tons i.e. six times larger than that of a proton gantry.

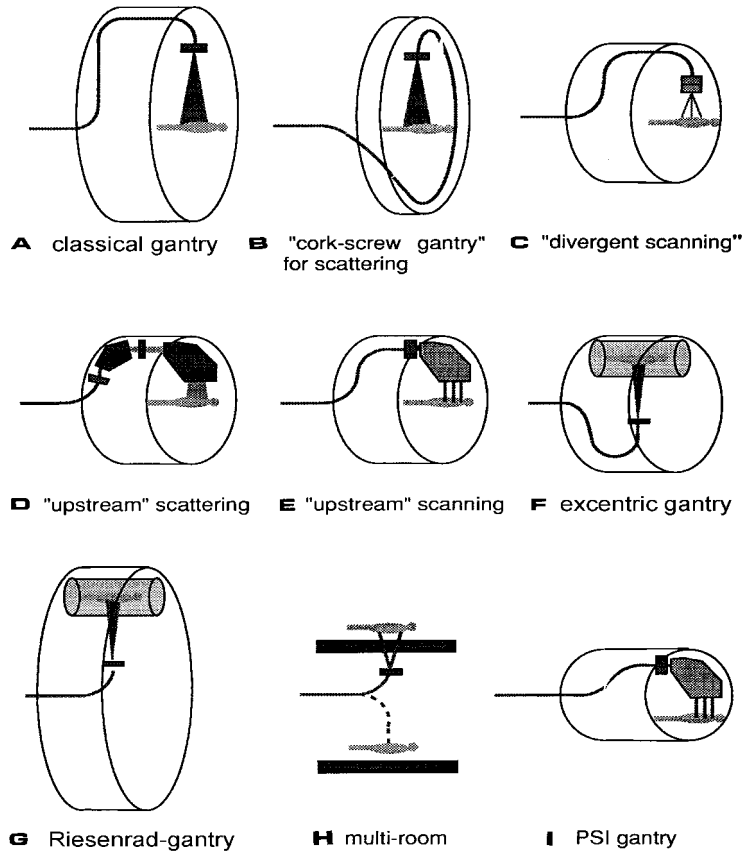

Figure 4.7: Classification of the different types of gantries proposed for particle therapy. (According to Pedroni 1994)

Because of these difficulties the idea of a gantry is frequently given up for future heavy ion therapy units in favour of a fixed-angle beam delivery of 45° or 90°. The possibility of superconducting gantries has been discussed. At Berkeley's Bevalac, patients were also successfully treated in a seated position. But this premises vertical CT scanners in order to diagnose the tumor under the same conditions, as it will be treated later on. It follows from the above that up to now there is no generally accepted solution for a gantry.

4.8 Accelerators

In the past, the therapy with heavy charged particles has mainly been promoted by physicists working at accelerators. Therefore, the question of the best accelerator for therapy was frequently in the centre of interest when it came to new facilities. However for optimum patient treatment, the discussion should start at the rear end i.e. with the patient, the number and indications to be treated and the kind of beam application. After these parameters have been decided the requirements for the necessary accelerator can be specified and given to the accelerator physicists and engineers.

For proton therapy, there seems to be no preference for cyclotrons or synchrotrons. Both types of accelerators have their benefits and shortcomings. Cyclotrons produce a very stable beam intensity that is suitable for beam scanning but the energy variation has to be performed with absorber systems. Cyclotrons are smaller but heavier than synchrotrons. Synchrotrons are generally more flexible and energy variation from pulse to pulse is easy. At present, both, cyclotrons and synchrotrons are used for proton therapy with good results.

For heavier ions like carbon, a synchrotron appears to be preferable since a cyclotron would become very heavy and probably more expensive than a synchrotron. In addition, synchrotrons are able to change the energy from pulse to pulse. Although a synchrotron is larger the empty space inside the magnet ring can be used for power supplies. In addition, the size of the accelerator becomes relative when compared to the space needed for the therapy rooms. The use of superconducting accelerators has also been discussed, especially in the Eulima project [Eulima 1991] but was given up because of the extended repair times of several days in case of an accelerator failure. One must keep in mind that patients have to be treated daily for 20 to 30 fractions. The closing of an accelerator for many days would be intolerable. Although the discussion on the best accelerators is still going on accelerator technology is presently at such a high level that any kind of accelerator will do.

4.9 Quality Assurance

A very important but frequently neglected problem of particle therapy is quality assurance. For particle therapy, quality assurance becomes the more important the more the precision and the efficiency of the beam are optimized. This was the case in the transition from conventional to particle therapy, which has a better dose profile. It is especially relevant for the target conforming beam scanning methods producing extremely sharp dose profiles. Here, the accuracy of the beam delivery has to be guaranteed by

extensive test procedures [Heeg 1998].

Quality assurance starts with the test of the beam quality i.e. its isotopic purity and energy, checks of the beam, spatial beam stability and finally the test of standard volumes irradiated in water phantoms. Thus, the fields produced can be compared to simple, planned fields. In addition, each treatment plan has to be verified in a water phantom. This is not at all trivial because the density inhomogeneities in the human body yield a different dose distribution than that of water. For control, the treatment plan has to be converted into a "water-equivalent" plan since only this water-equivalent plan can be controlled. Another difficulty arises for beam scanning when the field is constructed sequentially and when it is impossible to use thimble ionisation chambers that can be moved around in the field [Brusasco 1999].

The best quality control would be the measurement of the irradiated volume inside the patient. To some extent this is possible with the positron emission inside the patient's body being measured by means of PET [Enghardt 1999]. Although it is not yet possible to convert these PET images into dose distributions, the images indicate the stopping of the primary beam. This is especially relevant if the beam passes or stops close to critical structures.

In general, the greater efficiency of particle therapy also bears the risk of larger damage in case of misoperation but the technical progress provides better control systems for its prevention.

4.10 Therapy Facilities

4.10.1 History and Patient Statistics

In 1954 particle therapy started at the Lawrence Berkeley National Laboratory (LBNL) with the first proton treatment. Later also Helium and heavier ions were used at Berkeley. Most of the patients worldwide have been treated at the Harvard cyclotron which started 1961 and operates down to the present day. There was another proton treatment facility in Uppsala, Sweden, from 1957 until the accelerator was closed. It was then restarted in 1976. In France, two centers - one at Nice and one at Orsay - have been operating since 1991. In Russia, too, a large number of patients have been treated with proton therapy. Loma Linda was the first centre that was not based on an old physics machine but set up as a medically dedicated facility. With currently more than 1,000 patients per year it outnumbers any other facility.

In addition to the treatment of deep-seated tumors with 200 Mev protons there is also a very efficient program for the treatment of eye tumors. Here, 70 MeV is enough energy to reach the sufficient range of 2 cm. The most active centre for eye treatment is Optis at PSI, Villigen, with altogether more than 3,000 patients up to now. Also Clatterbridge, Nice and recently Berlin have set up very successful treatment facilities. The development for heavy ions is much slower than for protons. On the one hand, this is because the required accelerators are more expensive to build and to run and on the other hand, because the RBE problem had to be explored in its clinical aspects first.

Due to their extreme biological efficiency Berkeley started with Argon ions. But the very good tumor control was unfortunately linked to intolerable side effects. Consequently, Berkeley switched to lighter ions and treated approximately 400 patients with Neon. For radiobiological reasons, the heavy-ion therapy at NIRS, Chiba, began treatment with carbon ions right from the start, although it would have been possible to accelerate heavier ions up to Argon at the HIMAC. The therapy unit at Chiba is the first heavy-ion accelerator that is dedicated solely to therapy. It is the most complete system possible and consists of two large synchrotrons that are able to accelerate all kinds of ions from He to Ar.

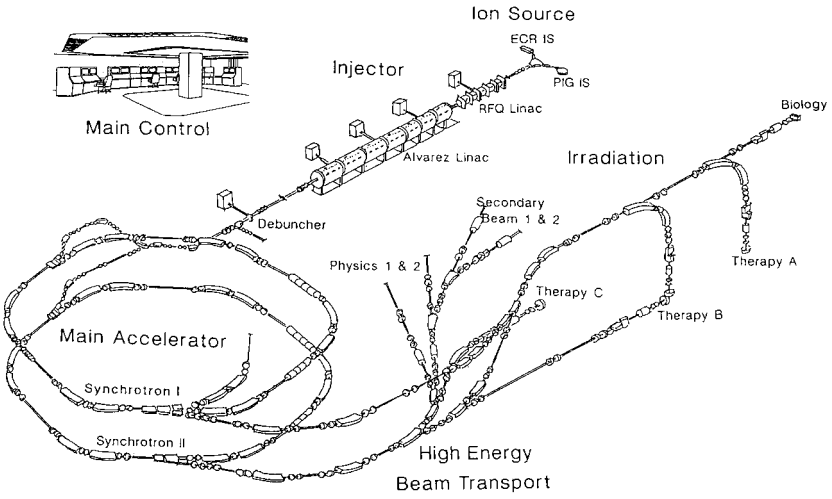

Figure 4.7: General layout of the HIMAC facility for heavy-ion treatment at Chiba, Japan [according to Amaldi 1997]

Table 1 WORLD WIDE CHARGED PARTICLE PATIENT TOTALS (Janet Sisterson, January 2001)

Who	Where	What	Date 1st RX	Date last RX	Recent Patient total	Date of total
Berkeley 184	CA. USA	p	1954	1957	30	
Berkeley	CA. USA	He	1957	1992	2054	June-91
Uppsala	Sweden	p	1957	1976	73	
Harvard	MA. USA	p	1961		8747	Jan-01
Dubna	Russia	p	1967	1974	84	
Moscow	Russia	p	1969		3268	June-00
St. Petersburg	Russia	p	1975		1029	Jun-98
Berkeley	CA. USA	HI	1975	1992	433	June-91
Chiba	Japan	p	1979		133	Apr-00
PMRC, Tsukuba	Japan	p	1983		629	Jul-99
PSI (72 MeV)	Switzerland	p	1984		3253	Dec-00
Dubna	Russia	p	1987		79	Dec-00
Uppsala	Sweden	p	1989		236	June-00
Clatterbridge	England	p	1989		999	June-00
Loma Linda	CA. USA	p	1990		5638	Dec-00
Louvain-la-Neuve	Belgium	p	1991	1993	21	
Nice	France	p	1991		1590	June-00
Orsay	France	p	1991		1894	Jan-01
N.A.C.	South Africa	p	1993		380	Nov-00
MPRI	IN USA	p	1993		34	Dec-99
UCSF - CNL	CA USA	p	1994		284	June-00
HIMAC, Chiba	Japan	HI	1994		745	Dec-99
TRIUMF	Canada	p	1995		57	June-00
PSI (200 MeV)	Switzerland	p	1996		41	Dec-99
GSI Darmstadt	Germany	HI	1997		72	June-00
HMI, Berlin	Germany	p	1998		166	Dec-00
NCC, Kashiwa	Japan	p	1998		35	June-00
					3304	ions
					28700	protons
				TOTAL	33104	all particles

Up to now, more than 700 patients have been treated at the HIMAC [Tsujii 1996]. The heavy-ion therapy unit at GSI, Darmstadt, is a small experimental set-up where the beam is available for patient treatment only three months a year. The main purpose of the facility is to demonstrate the clinical feasibility and reliability of newly developed techniques such as the intensity-controlled raster scanning, the biology-based treatment planning, the on-line PET and the control and safety systems. The intention is to transfer these techniques to a clinical therapy unit as soon as possible.

4.11 Future Plans

Another proton facility will be starting at Harvard University in the near future. Most of the new therapy units for heavy charged particles are being set up in Japan. Apart from Chiba, there are 4 new facilities being planned or under construction in Tsukuba, Kashiva and Wakasa. Hyogo started treatment only recently.

In Europe, there are several strong initiatives for heavy-ion therapy, that have been funded - at least partially - from their governments, for instance in Italy (TERA), Austria (Austron) and in Lyon, France. But also elsewhere new facilities will be constructed in the near future: In Lanzhou, China, a heavy ion facility including a therapy unit is under construction. In Germany, many plans for particle therapy are virulent as for instance in Munich, Erlangen and Regensburg but only the project at Heidelberg has been given high priority from the German Scientific Council. Because particle therapy has produced very good clinical results, many of the projects of Tab II have a good chance to be realized.

Table 2. *New facilities [Sisterson 2001]*

INSTITUTION	**PLACE**	**TYPE**	**1ST**
INFN-LNS, Catania	Italy	p	2001
NPTC (Harvard)	MA USA	p	2001
Hyogo	Japan	p, ion	2001
NAC, Faure	South Africa	p	2001
Tsukuba	Japan	p	2001
Wakasa Bay	Japan		2002
Bratislava	Slovakia	p, ion	2003
IMP, Lanzhou	PR China	C-Ar	2003
Shizuoka Cancer Center	Japan		2003
Rinecker, Munich	Germany	p	2003?
CGMH, Northern Taiwan	Taiwan	p	2001?
Erlangen	Germany	p	2002?
CNAO, Milan & Pavia	Italy	p, ion	2004?
Heidelberg	Germany	p, ion	2006
AUSTRON	Austria	p, ion	?
Beijing	China	p	?
Central Italy	Italy	p	?
Clatterbridge	England	p	?
TOP project ISS Rome	Italy	p	?
3 projects in Moscow	Russia	p	?
Krakow	Poland	p	?
Proton Development N.A. Inc.	IL USA	p	?
PTCA, IBA	USA	p	?

5. PROBLEMS OF RADIOPROTECTION IN SPACE

The problems of radiation protection in space are different from those in conventional radiation protection because the radiation in space mainly consists of heavy charged particles from protons to iron ions. These particles are delivered with energies far above the nuclear reaction threshold. Therefore, not only the primary particles but also cascades of secondaries contribute to the exposure of a space craft. There are two sensitive targets that are affected by the impact of radiation - man and computer. In the following, we will focus on the consequences for man and will not elaborate on such topics as for example semiconductor response which are beyond the capacity of the author and the scope of this contribution. Comprehensive reports on those problems of space radiation can be found for instance in [Majima 2000, Wilson 1991]

5.1 The Radiation Field

Depending on the distance from earth the composition of the radiation field varies because particles are trapped in the geomagnetic field. At low earth orbit (LEO), trapped protons and electrons from the radiation belt predominate (fig. 5.1).

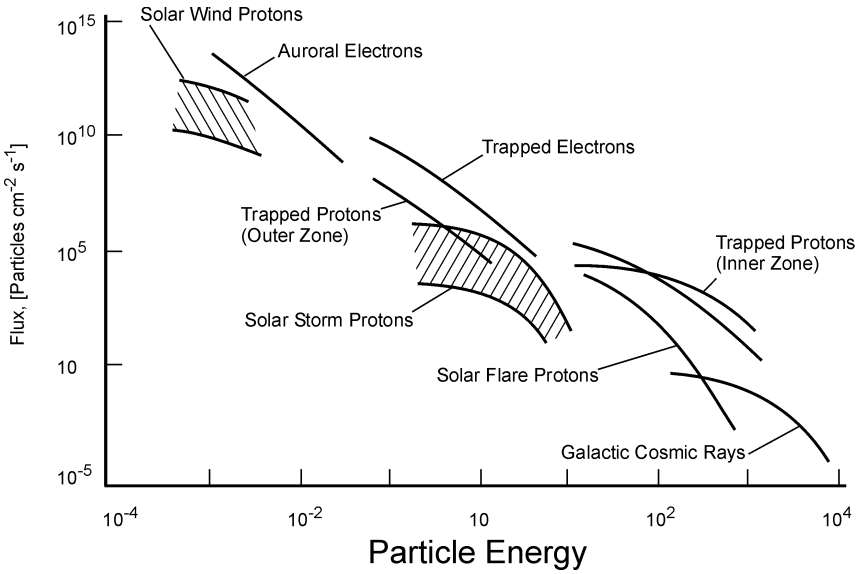

Fig. 5.1: Energy spectrum of the galactic cosmic radiation as function of particle energy in MeV (redrawn from J.W. Wilson 1991) .

Apart from the cosmic galactic rays there are also the protons of solar eruption events, the solar flairs. These solar particle events are statiscally distributed and cannot be predicted to occur or not to occur during a specific space mission. But in the long run, a stable period of eleven years for maximum solar activity has been observed. In solar particle events, a dose of a fraction of one Gray up to the Gray region can be delivered in a short time of a few hours or even less. Therefore, solar particle events could be life threatening in extreme cases but viewed on a long-term basis, they are so rare that they contribute only with a small fraction to the general radiation burden.

The main contribution of dose during a space mission outside the magnetic shielding of the earth originates from the galactic cosmic rays (GCR) (fig. 5.2). GCR are heavy charged particles from the most frequent protons up to iron ions. Ions heavier than iron are several orders of magnitude less frequent since they originate from super nova explosions and cannot be synthesized by exo-thermic nuclear fusion reactions like iron and the elements being lighter than iron.

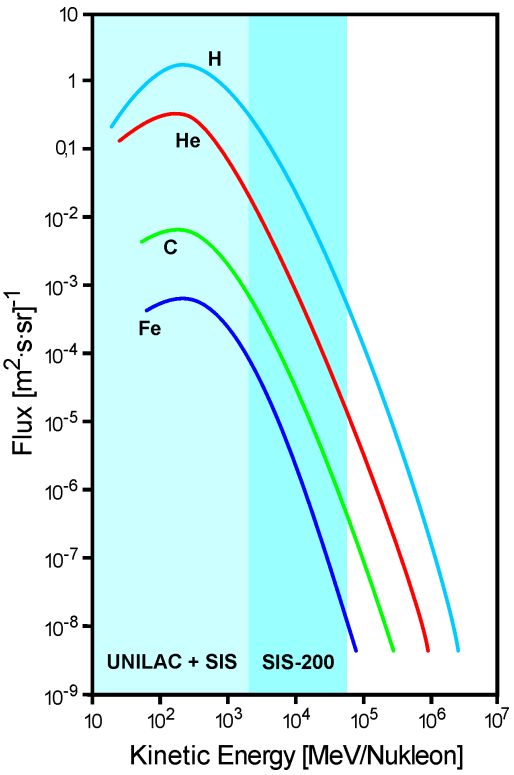

The galactic cosmic radiation has an energy spectrum with a broad maximum at a few hundred MeV per nucleon and a steep and continuous decay to-wards higher energies (fig. 5.2). This high-energy tail has been measured up to the TeV region and is a big problem for an effective shielding. Because the cross sections for nuclear fragmentation are still significant for the ions of these extremely high energies, any shielding layer introduced to stop the low-energy particles also produces showers of nuclear fragments from the high-energy particle impact.

Fig. 5.2: Energy spectrum of the galactic cosmic radiation (GCR) (adapted from Wilson 1991)

Transport calculations for the GCR spectrum in various shielding materials like aluminium showed that after a small benefit in the first thin shielding layers, thicker absorbers do not produce a net reduction of the biological effect that correlates reasonably with the increasing mass of the shielding material. The decrease in the amount of low-energy particles is almost compensated by the increase in nuclear fragmentation. For details of this very complex but important ion transport avalanches we ask the reader to refer to the comprehensive article by Wilson et al. 1991.

The fluence distribution of protons ranges over three orders of magnitude over Fe-ions but the energy deposition i.e. the dose of a single particle depends on the square of the atomic number. Therefore, the difference between protons and iron in their frequency contribution is nearly compensated by the dose. Taking the change in the relative biological efficiency into account the fraction of iron particles becomes as important as that of protons.

For low earth orbit (LEO), the total dose per day is about 1mSv behind a shielding of 1g/cm^2 of Aluminium. This is the average dose per year on earth. Spaceflights are on average 300 times more exposure-intensive than our daily life. But the actual value of a space mission very much depends on the altitude of the flight and on the inclination of the route. Because at the magnetic poles, shielding is drastically reduced and an orbit over the earth poles results in a greater exposure than an equatorial flight.

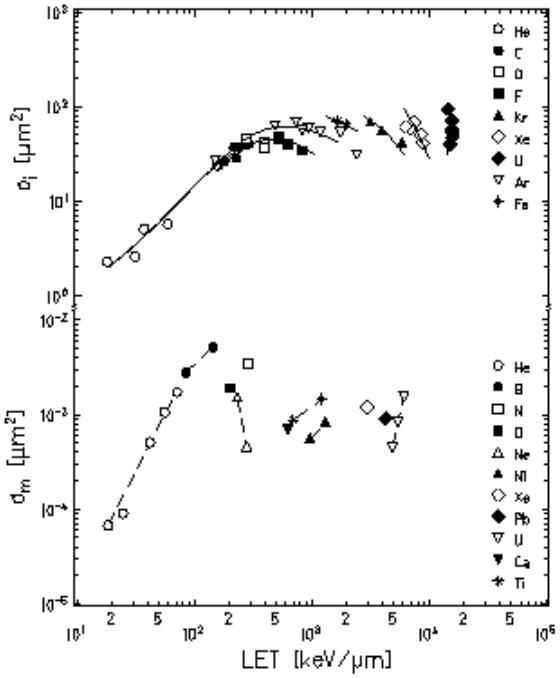

Figure 5.3
(top): Inactivation cross section of V79 Chinese hamster cells for various particles from He to U as a function of the linear energy transfer.

(bottom): Mutation cross section of the HGPRT gen in Chinese hamster cells as a function of the same parameters as above.
[according to Kiefer 1992]

Outside the geomagnetic shielding the particle composition of the GCR becomes more relevant and the estimation of the biological effect is determined rather by the hit probability of the critical target inside the cells, i.e. the cell nuclei, than by a dose averaged over a long time. For example, a three years' mission to Mars was calculated to produce 400 proton and 40 He-ion traversals through the nucleus of each cell of the human body. This number decreases for light ions to a hit probability of 3% for iron ions. According to this statistic, every cell nucleus will be hit by a proton once every three days and by a He ion once every thirty days. A human body consists of about 10^{14} cells. Concerning the high hit frequency and the large number of cells at risk it is very evident that a non-protracted exposure would be lethal while the distribution over a period of three years allows repair with a good chance to survive. However, the long-term consequences like cancer induction or genetic mutation determine the risk. It is known that a macroscopic tumor originates from one transformed cell. Concerning the high number of cells at risk it is obvious that most transformed cells are eliminated by the body's imuno-system. But if one mutated cell survives cancer will develop. Consequently, cancer is determined more by the biological processing than by mere induction statistics of DNA damage (fig. 5.3).

5.2 Genetic Effects and Cancer Induction

It is very difficult to make reliable and substantial statements concerning the biological consequences of human exposure to GCR. First the physical exposure cannot be predicted with sufficient accuracy because the physical i.e. the absorbed dose depends on the accidental exposure and its composition which cannot be predicted precisely. Even a retrospective analysis often lacks the necessary accuracy because it would request personal dosimeters to be carried by the astronauts that could give an analysis in atomic number and energy of all particles and the dose of other types of radiation.

On the biological side, the genetic mutation and cancer induction by radiation are very rare events in the range of 0,05 per Gray per person or less. This means for example that from a population of 10,000 people, irradiated with one Gray - which is just a third of the lethal dose - fortunately only a few hundred will develop cancer. This radiation-induced cancer has a latency of many years and becomes evident only within a long period of about 20 years. During this period many more cancer patients are diagnosed, who develop the disease due to other reasons than radiation. This was exactly the situation of the victims of the atomic bombing of Nagasaki and

Hiroshima where only after some years a measurable increase in the cancer incidence was found for leukemia but not for other cancer types because of the low incidence rate.

For ethical reasons, experiments inducing cancer in humans are not possible and even animal experiments are restricted and difficult to perform because of the large number of animals needed. Such experiments are mostly confined to sparsely ionising radiation. The data for Hiroshima and Nagasaki also refer to sparsely ionising radiation because the neutron component in both bombs contributed a few percent only.

Animal experiments with particle radiation are scarce and a straight-forward extrapolation from sparsely ionising radiation to particle exposure is yet impossible because we know that the biological response to densely ionising radiation is different from the X-ray response. An extensive synopsis of this problem was compiled by LBNL 1997 and by Nat Res. Council 1996.

With regard to the modelling of inactivation as shown in 3.2 one might consider a similar theoretical procedure for the calculation of the genetic or cancer risk. Starting from X-ray dose effect curves and the radial dose distribution in the track, the expected effect for particles should be determined. Such calculations were published [Wilson 1991] and represent the first reliable theoretical approach. However, the uncertainty of these calculations is large because of small probabilities and the complex biological mechanisms necessary to yield stable genetic mutations. In comparison to inactivation the cross section for mutations are three to four orders of magnitude smaller. For inactivation one could attribute the higher RBE values to the greater local ionisation density that impairs a successful repair of high fidelity (fig 5.3).

Stable genetic mutations are the result of a more complex biological process, that is, of a repair that was successful in terms of survival but not in terms of the fidelity of the genetic code. This means that all essential genes are still present but at least one of them in a mutated but still meaningful way. Therefore, an increase in local ionisation density causes a local increase in DNA damage, but these clustered DNA lesions at higher energy depositions are not necessarily correlated with a higher frequency for stable mutations.

The most complete set of mutation data on cellular level and for heavy particles concern the mutations of the HPRT gene. Without going into details on the relevance and limitations of these cellular data in comparison to the risk of a human being, the cross section given in fig. 5.3 clearly shows that, first, the absolute mutation cross section are 3-4 orders of magnitude smaller than the inactivation values. Second, the mutation cross sections for

heavier ions are smaller than for light ions indicating - in a still very crude way - that the mutation process is strongly determined also by other factors and not only by the primary ionisation density.

Similar results are reported for the induction of chromosome aberrations. Older measurements postulated a much lower incidence of chromosomal aberrations even for lighter ions. More recent experiments have shown that the expression time of heavy-ion-induced aberrations can be drastically delayed yielding low cross sections when analysed too early [Ritter 2000]. When time-integrated data are collected over longer intervals the number of chromosome aberrations as indicator of genetic effects has greater RBE values, indicating that heavy ions are more efficient in the initial stage of producing genetic damage. But in the course of time most of these aberrations lead to cell death and are therefore eliminated from the cell population. Mainly, aberrations from the translocation type i.e. aberrations where two DNA breaks are repaired with the wrong ends have a great chance to survive durably. Howerver, only a fraction of this aberration type might have biological consequences.

In addition to these genetic changes that become visible in the very next cell division after the exposure, a long-term genetic instability has been observed after particle exposure i.e. chromosome aberrations that become visible only after about 50 cell divisions but not earlier [Kadhim 1992].

From these considerations, the complexity of the risk estimation for GCR becomes evident. But because the general risk is small, upper limits have been fixed as a worst case scenario, as for instance the figure of an incidence rate of 0.05 per Gray for leukemia as given above.

6. CONCLUSIONS

The radiobiology of highly charged ions differs from the conventional radiobiology with photons because of the great local ionisation density that is produced along a particle track. From the primary data of energy loss and electron emission, the radial dose distribution inside a track can be calculated. In the center of the track, doses up to the Mega-Gray region can be found that decay with square of the radial distance from the center up to a maximum value given by the range of the most energetic electrons. Because of this very inhomogeneous dose distribution clustered DNA damage becomes more frequent that cannot be repaired by the cell. This yields a greater relative biological efficiency of particles compared to that of sparsely ionising radiaton. For cell inactivation the particle efficiency can be calculated by folding the X-ray dose effect curve with the radial dose

distribution of the particles. This method is used to calculate the killing efficiency in ion-beam treatment planning. Other parameters for treatment planning in ion-beam therapy are the pure physical data like beam lateral and longitudinal scattering and beam fragmentation.

From these data, dose distributions for cancer treatment can be achieved that are superior to any conventional therapy. In order to transform the planning into a therapy different beam application methods have been developed that allow - in its final and most sophisticated form - to reach a perfect congruence between planned and treated volume.

Using the small amount of radioactive positron emitters that are produced inside the patient's body, the beam delivery can be monitored from outside using positron emission tomography.

Because of the superiority of these treatment methods extremely good results in tumor therapy have been achieved. Up to now, approximately 30,000 patients have been treated, mainly with protons. And, a great number of projects for dedicated particle therapy centers are under way all over the world.

In space exploration, a major problem are the cosmic galactic rays that consist of highly charged ions from protons up to iron. Again, these particles have a greater biological efficiency than X-rays to induce genetic mutations and cancer. But the genetic processes are not only determined by the primary ionisation density but also by the biological response to the primary injury i.e. by the biological repair systems. Up to now, it is not possible to calculate the radiation risk in space with the desired accuracy. Because the energy spectrum of the GCR stretches up to very high values and because of the fragmentation process the application of absorber material is not only expensive but also - to a large extent - ineffective. Therefore, more accurate measurements and modelling is necessary to determine the radiation risk in space.

In general, particle radiobiology has reached a very microscopic understanding of the interaction of highly charged ions with living material. This knowledge can be used for a successful tumor therapy but for genetic changes the understanding is not sufficient to deliver exact data.

REFERENCES

Alonso, J.R., Synchrotrons: the American Experience, in: Hadrontherapy in Oncology, eds.: U. Amaldi, B. Larsson, Excerpta Medica Intercongress Series 1077, Elsevier 1994, 266-281

Amaldi U., The National Centre for Oncological Hadrontherapy at Mirasole, INFN, Frascati 1997

Barkas H.W., Nuclear Research Emulsions, Vol. I, Academic Press New York and London, 1963

Bethe H.: Zur Theorie des Durchgangs schneller Korpuskularstrahlung durch Materie, Ann. Phys. (Leipzig) (1930), 5, 325-400

Blakely E.A., Tobias C.A., Ngo F.Q.H., Curtis S.B., Physical and Cellular Radiobiological Properties of Heavy Ions in Relation to Cancer Therapy Application, in: Biological and Medical Research with Accelerated Heavy Ions at the Bevalac, eds.: M.D. Pirncello, C.A. Tobias, 1980, LBL 11220, 73-88

Blattmann H., Munkel G., Pedroni E., Böhringer T., Coray A., Lin S., Lomax A., Kaser-Hotz B. (1995) Conformal proton radiotherapy with a dynamic application technique at PSI, Progress in Radio-Oncology V, Ed. Kogelnik H.D., Monduzzi Editore, Bologna, 347-352

Bloch F., Bremsvermögen von Atomen mit mehreren Elektronen, Z. Phys. (1933a), 81, 363-376

Bloch F., Zur Bremsung rasch bewegter Teilchen beim Durchgang durch Materie, Ann. Phys. (Leipzig), 1933b, 5, 285-321

Bragg W., Kleemann R., On the α-Particles of Radium and their Loss of Range in Passing Through Various Atoms and Molecules, Phil. Mag. (1905), 10, 318-340

Brand H., Essel H.G., Herdel H., Hoffmann J., Kurz N., Ott W., Richter M., Therapy: Slow Control System, Data Analysis and on-line Monitoring, GSI Report 1998, 146-189

Brusasco C., A Detector System for the Verification of Three-Dimensional Dose Distributions in the Tumor Therapy with Heavy Ions, PhD Thesis Kassel 1999

Chu W.T., Ludewigt B.A., Renner T.R., Instrumentation for Treatment of Cancer Using Proton and Light-Ion Beams, Review of Scientific Instruments, Accelerator & Fusion Research Division, LBL-33403 UC-406 Preprint (1993)

Debus J., Haberer T., Schulz-Ertner D., Jäkel O., Wenz F., Enghardt W., Schlegel W., Kraft G., Wannenmacher M., Fractionated Carbon Ion Irradiation of Skull Base Tumors at GSI. First Clinical Results and Future Perspectives, Strahlenther. Onkol. 2000, 176, (5) 211-216

Enghardt W., Debus J., Haberer T., Hasch B.G., Hinz R., Jäkel O., Krämer

M., Lauckner K., Pawelke J., The Application of PET to Quality Assurance of Heavy-Ion Tumor Therapy, Strahlenther. Onkol. 1999, 175, Suppl. II, 33-36

Enghardt W., Fromm W.D., Geissel H., Keller H., Kraft G., Magel A., Manfraß P., Münzenberg G., Nickel F., Pawelke J., Schardt D., Scheidenberger C., Sobiella M., Positron Emission Tomography for Dose Localization and Beam Monitoring in Light Ion Tumor Therapy, Proc. Int. Conf. on Biological Applications of Relativistic Nuclei, Clermont-Ferrand, France, Oct. 1992, 30

Eulima: Cancer Treatment with Light Ions in Europe, Final Report, Geneva 1991

Friedländer E.M. Heckmann H.H., Relativistic Heavy-Ion Collisions Experiment, in: Treatise on Heavy-Ion Science, Vol 4, Ed.: D.A. Bromly 1985, 304-365

Gottschalk B., Koehler A.M., Schneider R.J., Sisterson J.M., Wagner M.S., Multiple Coulomb Scattering of 160 MeV Protons, Nucl. Instr. and Meth. 1992, B74, 467-490

Haberer Th., Becher W., Schardt D., Kraft G., Magnetic scanning system for heavy ion therapy, Nucl. Instr. and Meth. in Phys. Res. A 330, (1993), 296-305

Heeg P., Hartmann G.H., Jäkel O., Karger C., Kraft G., Quality Assurance at the Heavy-Ion Therapy Facility at GSI, Strahlenther. Onkol. 1998, 175, 36-39

Hüfner J., Heavy Fragments Produced in Proton-Nucleus and Nucleus-Nucleus Collisions at Relativistic Energies, Phys. Reports 1985, 125, 129-185

Jäkel O., Krämer M., Treatment planning for heavy ion irradiation, Physica Medica 1998, Vol XIV/1; 53-62

Kadhim M.A., Macdonald D.A., Goodhead D. T., Lorimore S.A., Marsden S. A. and Wright E. G., Transmission of chromosomal instability after plutonium alpha-particle irradiation, Nature 1992, 355, 738-740

Kiefer J., Heavy ion effects on cells: chromosomal aberrations, mutations and neoplastic transformation, Radiat. Environm. Biophys. 1992, 31, 279-288

Kraft G., Radiobiological effects of very heavy ions: inactivation, induction of chromosome aberrations and strand breaks, Nucl. Sci. Appl. 1987, 3, 1-28

Kraft G., Becher W., Blasche K., Böhne D., Fischer B., Gademann G.,Geissel H., Haberer Th., Klabunde J., K.-Weyrather W., Langenbeck B., Münzenberg G., Ritter S., Rösch W., Schardt D., Stelzer H., Schwab Th., The Heavy Ion Project at GSI, Nucl. Tracks Radiat. Meas. 1991, 19, 911-914, (Int. J. Radiat. Appl. Instrum. Part D)

Kraft G., Krämer M., Linear Energy Transfer and Track Structure, Advances

in Radiat. Biology 1993, Vol. 17, 1-52

Kraft G., Radiobiology of Heavy Charged Particles, in: Advances in Hadrontherapy, Eds.. Amaldi U., Larsson B., Lemoigne Y.; Excerpta Medica, Int. Congr. Series 1144, Elsevier 1997, 385-404

Kraft G., RBE and its Interpretation, Strahlenther. Onkol. 1999, 175, Suppl 2, 44-47

Kraft G., Scholz M., Bechthold U., Tumor Therapy and Track Structure, Radiat.Environm.Biophys. 1999, 38, , 229-237

Kraft G., Kraft-Weyrather W., Taucher-Scholz G. and Scholz M., What Kind of Radiobiology should be done at a Hadron Therapy Center, Advances in Hadrontherapy, Proceedings of the International Week on Hadrontherapy, European Scientific Institute, Archamps, France, 20-24 November 1995 and of the Second International Symposium on Hadrontherapy, PSI and CERN, Switzerland, 9-13 September 1996

Kraft G.,Tumor Therapy with Heavy Charged Ions, Progr. Part. Nucl. Phys. 2000, 45, 473-544

Krämer M., Kraft G., Calculations of Heavy Ion Track Structure, Radiat. Environm. Biophys. 1994, 33, 91-109

Langen K.M., Jones T.L., Organ Motion and its Management, Int.J.Radiation Oncology Biol. Phys. 2001, 50, 265-278

LBNL Report, Modelling Human Risk: Cell and Molecular Biology in Context, LBNL Report 40278, 1997

Majima H.J., Fujitaka K. (eds), Exploring Future Research Strategies in Space Radiation Science, Proceedings of the 2nd International Space Workshop Feb. 16-18, 2000, Chiba NIRS 2000

Molière G., Theorie der Streuung schneller geladener Teilchen II, Mehrfach- und Vielfachstreuung, Z. Naturforschung 1948, 3a, 78-97

National Research Council: Radiation Hazard to Crews of Interplanetary Missions - Biological Issues and Research Strategies, National Academy Press, Washington 1996

Pedroni E., Beam Delivery in Hadrontherapy in Oncology, Excerpta Medica 1994, eds. U. Amaldi, B. Larsson, 434-452

Reinhold C.O., Schultz D.R., Bechthold U., Kraft G., Hagmann S., Schmidt-Böcking H., Ternary ridge of ejected electrons from fast ion-atom collisions, Physical Review A 1998, 58, 3, 2611-14

Renner T., Nymann M., Singh R.P., Control Systems for Ion Beam Radiotherapy Facilities, in: Ion Beams in Tumor Therapy, ed.: U. Linz, Chapman & Hall, 1995, 156-265

S. Ritter, E. Nasonova, E. Gudowska-Nowak, M. Scholz, G. Kraft, High-LET-induced chromosome aberrations in V79 cells analysed in first and second post-irradiation metaphases, Int. J. Radiat. Biol. 2000, 76, 149-161

Schlegel W., Pastyr O., Bortfeld T., Gademann, G., Menke M., Maier-Borst

W.,Stereotactically Guided Fractionated Radiotherapy: Technical Aspects, Radiother. Oncol. 1993, 29, 197-204

Scholz M., Kraft G., Calculation of Heavy Ion Inactivation Probabilities Based on Track Structure, X-ray sensitivity and target size, Radiat. Prot. Dosimetry, (1994), Vol. 52, Nos 1-4, 29-33

Scholz M., Kellerer A.M., Kraft-Weyrather W. and Kraft G., Computation of Cell Survival in Heavy-Ion Beams for Therapy. The Model and its Approximation, Radiat.Environ.Biophys.,1997, 36, 59-66

Sisterson J.: Particles, A Newsletter for those Interested in Proton Light Ion and Heavy Charged Particle Radiotherapy, 28/2001, 13-14

Tsujii H., Preliminary Results of Phase I/II Carbon Ion Therapy at NIRS, Int. Part. Therapy Meeting and XXIV. PTCOG Meeting, April 24-26, Detroit Michigan 1996

Verhey L.J., Comparison of achievable Dose Distributions Using Gamma Knife, Protons and IMRT, in: Intensity-Modulated Radiation Therapy, Ed: E.S. Sternik, Advanced Med. Pub. 1997, 127-142

Wambersie A., The Future of High-Let Radiation in Cancer Therapy, in: Chauvel P. and Wambersie A., Eulima Workshop on the Potential Value of Light Ion Beam Therapy, Publication No. EUR 12165, Commission of the European Community, Brussels, 1989

Weber U., Volumenkonforme Bestrahlung mit Kohlenstoffionen, PhD-Thesis, Universität Gh Kassel, 1996

Weyrather W.K., Ritter S., Scholz M., Kraft G., RBE for Carbon Track Segment Irradiation in Cell Lines of Differing Repair Capacity, Int. J. Radiat. Biol 1999, 11, 1357-1364

Wieszczycka V., Preliminary Project of a Polish Dedicated Proton Therapy Facility, Ph.D Thesis 1999, Warsaw, 194-198

Wilson R.R., Radiological Use of Fast Protons, Radiology 1946, 47, 487-491

Wilson, J.W. et al., Transport Methods and Interactons for Space Radiations, NASA 1991, Publication 1257